AD-A132 401 REFLECTION AND IDENTIFICATION STUDIES APPLIED TO TERRAIN IMAGING RADAR(U) MICHIGAN UNIV ANN ARBOR DEPT OF GEOLOGICAL SCIENCES P L JACKSON 30 JUN 83 ETL-0331 1/1

UNCLASSIFIED DAAK70-82-C-0100 F/G 17/9 NL

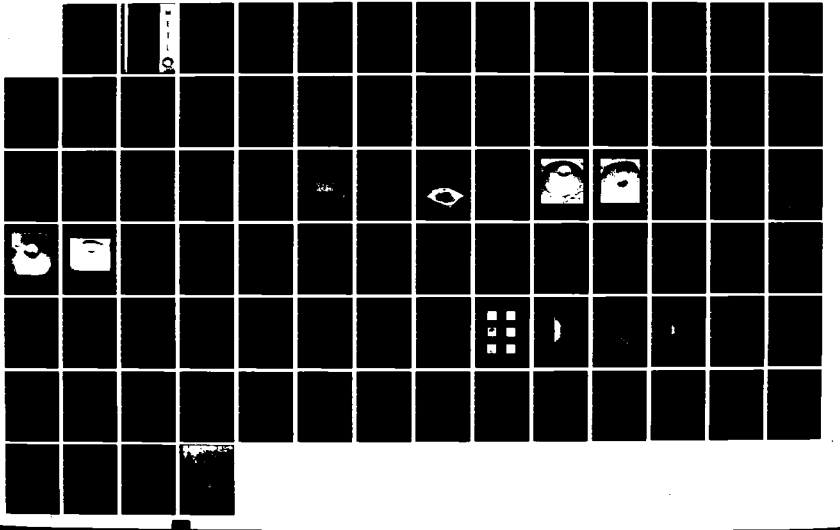

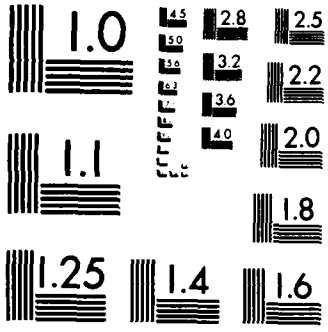

(2)

ETL-0331

Reflection and identification studies applied to terrain imaging radar

Philip L. Jackson

The University of Michigan
1006 C.C. Little Bldg.
Ann Arbor, MI 48109

June 1983

Prepared for

U.S. ARMY CORPS OF ENGINEERS
ENGINEER TOPOGRAPHIC LABORATORIES
FORT BELVOIR, VIRGINIA 22060

E T L

US ARMY ENGINEER TOPOGRAPHIC LABORATORIES
ETL

Destroy this report when no longer needed.
Do not return it to the originator.

The findings in this report are not to be construed as an official Department of the Army position unless so designated by other authorized documents.

The citation in this report of trade names of commercially available products does not constitute official endorsement or approval of the use of such products.

Unclassified

SECURITY CLASSIFICATION OF THIS PAGE (*When Data Entered*)

REPORT DOCUMENTATION PAGE		READ INSTRUCTIONS BEFORE COMPLETING FORM
1 REPORT NUMBER ETL-0331	2. GOVT ACCESSION NO AD-A132 401	3 RECIPIENT'S CATALOG NUMBER
4 TITLE (*and Subtitle*) Reflection and Identification Studies Applied to Terrain Imaging Radar		5 TYPE OF REPORT & PERIOD COVERED Contract Report 6/11/82 - 6/11/83 6. PERFORMING ORG REPORT NUMBER
7 AUTHOR(*s*) Philip L. Jackson		8. CONTRACT OR GRANT NUMBER(*s*) DAAK70-82-K-0100
9 PERFORMING ORGANIZATION NAME AND ADDRESS Department of Geological Sciences The University of Michigan, 1006 C.C. Little Bldg. Ann Arbor MI 48109		10 PROGRAM ELEMENT PROJECT TASK AREA & WORK UNIT NUMBERS
11 CONTROLLING OFFICE NAME AND ADDRESS U.S. Army Engineer Topographic Laboratory Research Institute, Bldg 2592 ATTN ETL-RI-D, Ft. Belvoir VA 22060		12. REPORT DATE 6/30/83 13. NUMBER OF PAGES 78
14. MONITORING AGENCY NAME AND ADDRESS (*if different from Controlling Office*)		15. SECURITY CLASS. (*of this report*) Unclassified 15a DECLASSIFICATION/ DOWNGRADING SCHEDULE

16. DISTRIBUTION STATEMENT (*of this Report*)

Approved for public release; distribution unlimited

17 DISTRIBUTION STATEMENT (*of the abstract entered in Block 20, if different from Report*)

18. SUPPLEMENTARY NOTES

19 KEY WORDS (*Continue on reverse side if necessary and identify by block number*)

Radar Backscatter
Synthetic Aperture Radar
Fourier Transform
Terrain Identification
Slope Effects

20. ABSTRACT (*Continue on reverse side if necessary and identify by block number*)

Two separate studies were undertaken. The first was concerned with the slope effects on backscatter of synthetic aperture radar (SAR). The imagery of a cinder cone (SP Mountain in northern Arizona), which has near-homogeneous surface roughness, was studied. The flight parameters of the imaging radar vehicle were found from the radar image and topographic data obtained from a 1:62500 map. The slant range radar image was converted to ground range with relief displacement rectified. The three-dimensional angle of incidence for

DD FORM 1 JAN 73 1473 EDITION OF 1 NOV 65 IS OBSOLETE

Unclassified

SECURITY CLASSIFICATION OF THIS PAGE (*When Data Entered*)

Block 20 continued:

each element was computed and plotted against the backscatter value. The average backscatter curve was a typical S-shaped pattern. With the techniques developed for the above, pseudo-SAR slant and ground range images were generated from the topographic data. The second study was concerned with investigating discrimination techniques for uncultivated, agricultural, suburban and urban areas. The work was limited to the use of the Fourier transform. Optical transforms and Fast Fourier transforms were obtained of optically processed SAR imagery. This preliminary work showed distinct differences between uncultivated and cultural areas, but not between cultural areas.

PREFACE

This document was prepared under Contract No. DAAK70-82-C-0100 for the U,S, Army Engineer Topographic Laboratories, Fort Belvoir, Virginia 22060 by The Unviversity of Michigan, Ann Arbor, Michigan. The Contracting Officer's Representative was Mr. Richard A. Hevenor.

The SAR data of SP Mountain was flown by ERIM, Ann Arbor, Michigan, for the U.S. Geological Survey, Branch of Astrogeologic Studies, Flagstaff, Arizona, on October 20, 1978, and generously made available for this study.

TABLE OF CONTENTS

Appendices, Fortran Programs:

LIST OF FIGURES

PART ONE

INTRODUCTION

Local angles of incidence severely affect radar images of the terrain. Angles between the direction of radar propagation and the normal to the local tangent plane of radar-imaged terrain can be visualized readily in Figure 1.

Slope affects the radar backscatter along with two other parameters: the roughness of the surface, and the dielectric constant of the surface materials. These three characteristics of a surface control the amount of radar backscatter. Since they simultaneously affect the image, they are difficult to delineate. A brightness change in the image, for example, might be caused by a surface change in one, two, or all three of these surface characteristics. It is diagnostic of the surface to ascertain whether an image characteristic is caused by the slope, the roughness, or the composition of the surface material. A means of isolating one of the individual characteristics would enable improved interpretation of the terrain since one could then better interpret the effect of the other two.

The characteristic investigated here is slope.

When the effects of the slope are known, effects of surface roughness and composition (dielectric constant) can then be more definitely interpreted.

Slopes can be found from topographic data, which exist in several forms for the United States and in some other regions. Also elevation data can be found from stereo radar, but this report is confined to using topographic data

for this purpose.

The first thing which must be done to match the radar backscatter with the local slope is to convert the slant range radar representation to ground range (map coordinates). In this way the backscatter for each image pixel can be correlated with the slope found from the topographic data.

This correlation, however, is complicated by radar relief displacement. Figure 2 shows a simple and a complicated case of slant to ground range distortion. In the complicated case with relief displacement elevated areas are displaced toward the radar vehicle. This displacement must be removed in the image. The rectification of this relief displacement has been accomplished recently by the author and colleagues (Rawson et al.,1981).

Conversion of slant range to ground range, including relief displacement, enables the assigning of incidence angles to each pixel of the radar image. The gradient of topographic data represented in a two-dimensional array can be found readily by the difference in array element values in the east-west and north-south directions. The incident angle lies between the direction of the gradient (which is normal to the local tangent plane of the terrain) and the direction of radar propagation.

Radar backscatter from each location is then plotted against the angle of incidence to obtain a plot similar to those found in Cosgriff, et al.(1960). Plots obtained by

the procedure described here are, however, produced from actual SAR flights, and can be used both to determine backscatter and also to interpret surfaces.

SP Mountain in Northern Arizona was chosen to use as an image in the development of this technique (See Figure 3). Much of the mountain approximates portions of a right circular cone. It presents slowly changing gradients under conditions of surface roughness which are close to uniform. "Uniform" is a relative term, and a variance is to be expected in the backscatter data. The roughness of the surface, however, is not dependent on the angle of incidence as all sides and elevations on the side of the mountain are essentially identical in composition and surface roughness.

To obtain an accurate ground range image the flight parameters must be accurately known. An aircraft usually uses barometric pressure, subject to inflight variations, to measure altitude. Absolute altitude is often in gross error. To more accurately determine the flight parameters, three techniques can be used to fix the position of the radar vehicle. The first requires two control points and the knowledge of the absolute slant range. The second requires three control points on a range line. The third requires several iterations along one or a few range lines at different altitudes to find the altitude for the best fit of computed ground range configurations to map features.

Since the required computation for removing relief displacement appeared similar to that of constructing

pseudo-SAR images, an algorithm and program was devised for this purpose. The pseudo-reflectivity of the test example was based upon the backscatter vs. angle-of-incidence analysis found with SP Mountain. Both slant-range and ground-range pseudo-SAR representations of SP Mountain were generated.

The approach toward obtaining backscatter vs. angle-of-incidence plots are presented in this section, including the methods, algorithms, computer programs, and examples in the form of plots or images.

BACKGROUND

The purpose of this work is to develop a method to isolate the slope-dependence in side-looking radar images of the terrain. With such a method the effect of slope could be minimized in a resulting image. Also, for regions of near-uniform roughness the effect of slope could be found.

From ground-based experiments Cosgriff et al.(1960) found the typical plot to be S-shaped. It is, of course, higher the lower the angle-of-incidence becomes. Using the reference of normal incidence as 0 degrees, the typical curve is steep for about 20 degrees, flattens for about the next 30 - 50 degrees, and becomes steep again within the last 20 degrees or so. Figure 4 shows a generalized backscatter curve which is similar to those in Cosgriff et al.(1960).

Although the general shapes of the curves are similar,

they vary for different types of surfaces. Most scenes have heterogeneous surfaces, so a general curve to fit all surfaces cannot be found. Also, on the most homogeneous of surfaces one would expect to find variations in the backscatter data. Unfortunately, Cosgriff et al., although they have many groundbased experimental plots, do not discuss or present the scatter (or variance) they found in gathering these data.

If the angle of incidence can be found and approximately compensated for, the effect of slope can be attenuated by using an approximate backscatter curve for the region of assumed terrain type. The resulting radar image would then be made more responsive to surface roughness and composition of the terrain material.

For an example in a different context, a use of the backscatter response was made with Seasat SAR and Space Shuttle SIR A data, both over the same area (Ford, et al., 1983). The Seasat imagery was obtained at an average angle-of-incidence of 20 degrees, the SIR A an average of approximately 50 degrees. Due to the S-shaped curve mentioned above, the SIR A data were affected relatively little by slope changes within its 40° to 70° angle of incidence range, while the Seasat data were affected relatively severely by slope changes within its 15° to 25° incidence angle range. To exploit this difference the Seasat data was reproduced with color coding for intensity of backscatter, and the brightness of this color coded image

was modulated by the intensity in the SIR A image. In this way the S-shape of the backscatter curve was attempted to be exploited. The color was weighted toward topography, the brightness toward small-scale roughness

The approach taken here is to convert slant range to ground range, so that each pixel in the radar image relates to a known terrain location. The gradient at the terrain location is then computed from known topographic data, and the angle between the direction of the gradient and the incident radar beam found. To achieve this correlation between the SAR image pixel and the ground location requires accurate knowledge of the vehicle flight parameters of altiutde and groundtrack.

Flight parameters are found with discrete control points on the image and map, or by iterative computation along one or a few range lines until the ground range conversion matches the topographic map.

With accurate flight parameters, the distances from each terrain sample to the radar vehicle can be found, as both the sample location and the vehicle location are known. The brightness at that slant range distance is then assigned to the ground range (or map location) along each range line in the image.

To find the ground range, it is first necessary to establish a digital array whose elements correspond to map locations. Elevation values are stored in each element of the array. X-Y locations are digitized along the contours

of a topographic map placed on a tablet digitizer. Enough elevation data points are digitized so that all array elements can be filled in. The filling-in is accomplished first by a nearest neighbor routine, and then by averaging over a cluster of points.

After assigning the backscatter values to each element of the ground range array, the gradient is computed by taking differences in the elevation in the east-west and north-south directions. The angle between the incident radar beam and the direction of the gradient is then computed. This angle is, of course, the angle of incidence, as the gradient direction is the normal to the local plane of the surface. Knowing the backscatter and the angle of incidence at each location enables one to construct backscatter curves.

The backscatter curve can then be plotted. This is done by a scatter plot, in which a dot is plotted for each location on the map. On the plot the abscissa is the angle of incidence and the ordinate is the intensity of backscatter.

To check the above process, an expression for the backscatter can then be formulated, and pseudo-SAR images constructed from the topographic data. Pseudo-images can be used for radar flight planning.

These processes are discussed in more detail in the following sections.

THE EXPERIMENTAL SITE

For this experiment radar imagery was needed of a site which would enable backscatter angles to be extensively compared on a surface with uniform roughness. The geometery of the site also must be such that distortions are obvious. Most mountainous and hilly terrain is not suitable for this purpose because of the irregularity of surface slopes, and the heterogeneity of surface roughness. A symmetrical cone with uniform roughness would be suitable, providing almost laboratory-like control of angle of incidence as well as uniform surface roughness. Also the geometry would aid in revealing distortion in the slant to ground range converted images.

SP Mountain in Northern Arizona closely fulfills these needed attributes. Located at 35^{o} 35' N, 111^{o} 38' W, in Township 25N Range 7E, Section 3, SP Mountain is a cinder cone. The cone is 260 m high with a diameter of 1.2 km. It closely approximates a right circular cone with a slope of approximately 29 degrees. The flanks of SP Mountain have a surface of "...a fragmental agglutinate of balsatic cinders...[and] scoria..." (Schaber et al.,1980). Scoria is defined as

> "Volcanic Slag: Pyroclastic ejecta, usually of basic composition, characterized by marked vesicularity, dark color, heaviness, and a texture that is partly glassy and partly crystalline. Fragments of scoria between 4 mm and 32 mm are essentially equivalent to volcanic cinders." (American (Geological Institute Dictionary, 1975).

Except for the base of the cone, where coarse (10-30 cm) fragments have accumulated (Schaber,1980), the surface of the mountain is essentially homogeneous, and its variation in roughness is statistically equivalent on all flanks of the cone.

At the summit of the mountain is a crater 400 m in diameter and 120 m deep. This portion of the mountain, however, is not used for backscatter studies, because the surface roughness may be different, and the edges of the crater are sharper than the contour sampling would accomodate.

The SAR image was obtained during a flight on October 20, 1978, sponsored by the U.S. Geological Survey, Branch of Astrogeologic Studies, Flagstaff, Arizona. The X-Band like-polarized (HH) data were optically processed and subsequently digitized.

DIGITIZING OF TOPOGRAPHIC DATA

Although DMA digitized topographic data is available for the United States, both the horizontal and elevation sampling intervals were found to be too coarse for this experiment. At this latitude the sampling interval is approximately 65 m. The topographic data were therefore directly digitized from topographic maps, and represented in an array with 12 m spacing.

SP Mountain topographic data were digitized on a Hitachi Data Tablet Digitizer Model HDG-3648 B/L from a USGS 1:62500

map with 40-foot contour intervals (no 1:24,000 map is available). 1171 points were digitized in an area representing slightly less than 1.2 x 1.2 km on the terrain. The digitized output from this process was a series of 1171 triplets consisting of the horizontal position, vertical position, and elevation. The spatial accuracy of the digitizing was specified by the manufacturer to be 1/1000 in.

Two steps were used to convert the sequential data representation into a two-dimensional array representation. In the first, a nearest-neighbor method, the elements of a 100x100 two-dimensional array were assigned map locations. The uniformly spaced array elements refer to specific locations spaced 12 meters apart on the terrain. The elevation data found with the tablet digitizer were irregularly spaced within the terrain area represented by the array. The digitzed elevation value at a location found closest to an array element location ("nearest neighbor") was assigned to this element. The second step was the averaging of the elevations found within a 3 x 3 matrix about the element. The program for these operations is listed in Appendix A.

A perspective plot constructed from the array topographic data of SP Mountain is shown in Figure 5. Note that the slopes of the flanks of the mountain are accurate, but the edges of the crater at the top of the mountain are rounded off due to the averaging.

The flanks of the mountain are accurately represented because the spatial frequency is low on this portion of the mountain. This portion of the data is satisfactory for this experiment because it presents a relatively large area of continuously changing incidence angles from approximately 20 degrees to 80 degrees. This area also has statistically homogeneous surface roughness. Moreover, the edges and interior of the summit crater may present a different surface roughness. An annulus circling the mountain is the optimal area for the determination of backscatter.

On a 100 x 100 grid approximately 2500 samples fall on the flanks of the mountain a sufficient distance from the top so that negligible distortion of slope occurs. The depressed areas at the upper and lower right corners and in the middle near the left edge are the data samples that were not filled in by the smoothing.

Figure 6 is a contour plot made from the digitized array data; for comparison, see Figure 3, a blowup (to 1:16560) of the USGS 1:62500 map.

Digitized radar data for this area were also placed in a 100 x 100 array. The data were originally recorded with 1.5 meter sampling interval. To obtain 12 meter sampling intervals the radar data was smoothed by a "star" array (an average of 18 data samples, 9 in the x-direction and 9 in the y-direction). A reconstruction of the radar image from the smoothed 100 x 100 array is shown in Figure 7.

REMOVAL OF RELIEF DISPLACEMENT

Relief displacement rectification with known topographic data can be accomplished in a straightforward fashion. Given the flight parameters (altitude and groundtrack) one simply measures the distance from a location on the terrain to the radar vehicle. this distance is simply

$$R = (g^2 + (h-e)^2)^{1/2}$$

where h is aircraft altitude, e is local elevation, R is slant range, and g is ground range. One then assigns the backscatter value at the slant range location R to the corresponding round range location. These elemental operations complete the process of slant to ground range conversion with relief displacement. A Fortran program for this purpose is listed in Appendix B. Details such as using nearest neighbor, interpolation, and the kind and sophistication of interpolation occur, but are not basic to the process. Also, the position of the radar vehicle must be accurately known.

The ground range image of SP Mountain with relief displacement removed is shown in Figure 8.

Vehicle position is often inaccurately measured during flight. Aircraft altitude, for example, is taken from barometric data at a regional airport usually at some distance, and, of course, the barometric pressure can change during flight.

DETERMINATION OF AIRCRAFT PARAMETERS

Slant-to-ground range conversion with relief displacement is extremely sensitive to the altitude and ground track of the radar vehicle. Inaccuracies in these two parameters can prevent accurate estimation of ground range.

Altitude of aircraft is usually recorded by barometric pressure, the reference for which is taken from a regional center. The purpose of the altitude measurement is safety, so that positional relationships between aircraft are known. The absolute altitude is not required for this purpose.

In the case of the SP Mountain imagery, the reference barometric pressure was taken in Albuquerque, New Mexico, and the image was obtained in Northern Arizona during the passage of a storm front. The recorded altitude was 21,000 ft (6401 m). Attempts at converting the SP Mountain slant range image to ground range using 6401 m altitude resulted in ground range images which did not fit the map coordinates. It was then necessary to devise means to fix the aircraft altitude and ground track so that a more accurate ground range estimation could be made.

Since conspicuous features are apparent on both the slant range imagery and the contour map, control points can be established along range lines, and the correspondence between the image and the map can then be used for determination of the aircraft parameters. Three methods can be used. Computer programs for these three methods are

listed in Appendix C.

Method 1

The first method is very simple. For this method the absolute slant range must be known. As seen in Figure 9 we know the lengths of three sides of a triangle (R_1,R_2,G_{1e}), and the precise location can be found. The vertex defines the position of the aircraft. The altitude h and groundtrack location g can be found as follows:

From Figure 9

$$h = R_1 \sin \theta,$$

$$g = R_1 \cos \theta,$$

where h is the aircraft altitude,

g defines the ground range,

R_1 is the slant range to the nearest control point,

R_2 is the slant range to the farthest control point,

$\alpha = \arctan (e/\Delta G_1)$,

$\Delta G_{1e} = \Delta G_1 \sec \alpha$

e is the elevation difference between points,

$\beta = \arccos((R_1^2 - R_2^2 + \Delta G_{1e}^2)/2R_1\Delta G_{1e})$,

and $\theta = 180 - \beta - \alpha$ degrees.

Method 2

The second method can be applied when the absolute value of the slant range is not known (when only ΔR, ΔG and e are known). As shown in Figure 10, θ_1, the depression angle of a bisector line, can be found. The crossing of two such bisector lines establishes the aircraft location.

The vehicle must be on the bisector line, because ΔR

must be maintained between the slant ranges to the near and far control points. If the vehicle were above or below the bisector line the difference between the two slant ranges would change, violating the condition of ΔR being a constant. We can therefore choose arbitrary values for R_1 and R_2. Operations identical to those in method 1 can then be used to find the interior angles designated by indexed β and γ.

Using the nomenclature of Figure 10,

$$\theta_1 = 180 - \beta_1 - \alpha_1 - \gamma_1/2 \text{ degrees},$$

$$\Delta G_e = 0.5([e_2-e_1]^2 + [\Delta G_2-\Delta G_1]^2)^{1/2},$$

$$\alpha_3 = \arctan([e_2-e_1]/[\Delta G_2-\Delta G_1]),$$

$$R_b = \Delta G_e \sin\beta_4/\sin(180-\beta_3-\beta_4),$$

$$h = R_b \sin\theta_1 + 0.5e_2,$$

and $$g = h \tan\theta_1 - 0.5\Delta G_1.$$

The flight altitude h and ground range g define the flight parameters.

Method 3

The third method is simply to probe for the correct altitude, knowing the slant range to one control point. The probing is accomplished by taking one range line, and converting the slant range to ground range iteratively for different vehicle altitudes. As the slant range is known, and the altitude is assumed, only one groundtrack can be found for each assumed altitude.

The ground range for each altitude is then compared with the map. The altitude for which the ground range most

closely corresponds to the map is then taken as the accurate altitude.

Using method 3 for the SP Mountain imagery the altitude was found to be 6100 m, a difference of 301 meters from the 6401 m altitude found with barometric pressure.

ANGLES OF INCIDENCE

Once ground range and the position of the radar vehicle are accurately established, backscatter vs. angle of incidence values can be computed. For each data sample the backscatter value in the form of a greytone is known from the SAR image, and the gradient of the local tangent plane can be found by using nearby samples. The angle between the radar beam and the normal to the local tangent plane defines the incident angle.

The normal to the tangent plane can be found as follows: Find the difference in elevation between topographic data samples on either side of the data sample for which the tangent plane is to be found. Divide this elevation difference by the distance between the two differenced samples. This will give an approximation of $\partial Z/\partial X$.

Performing the same operation with the elevation difference found from two corresponding samples in the along track direction will give an approximation of $\partial Z/\partial Y$.

These two approximations of partials determine the normal to the local tangent plane, the direction cosines of which are:

$$l_1 = 1/D_1;\ m_1 = (\partial Z/\partial X)/D_1;\ n_1 = (\partial Z/\partial X)/D_1$$

where $D_1 = (1 + [\partial Z/\partial X]^2 + [\partial Z/\partial Y]^2)^{1/2}$

Since the position of the radar vehicle is known, as well as the location of the sample data point, the direction of the incident radar beam can then be determined. The direction cosines are

$$l_2 = (h-e)/D_2$$

and $m_2 = G/D_2$

where $D_2 = ((h-e)^2 + g^2)^{1/2}$.

The angle of incidence at each sample point is, as previously stated, the angle between the incident radar beam and the normal to the local tangent plane. The analytic geometry formula for the angle ϕ between two lines in three-dimensional space is

$$\text{Cos } \phi = (l_1 l_2 + m_1 m_2 + n_1 n_2)/D_1 D_2$$

where l_i/D_i, m_i/D_i, and n_i/D_i; i=1,2, are direction cosines,

$$D_i = (l_i^2 + m_i^2 + n_i^2)^{1/2};\ i=1,2,$$

and subscripts 1 and 2 refer to the two lines.

This expression becomes, in radar and terrain coordinates,

$$\phi = \text{Arccos}((g\partial Z/\partial X + (h-e))/AB)$$

where $A = (1 + (\partial Z/\partial X)^2 + (\partial Z/\partial Y)^2)^{1/2}$

and $B = (g^2 + (h-e)^2)^{1/2}$

One computes this angle ϕ for each pertinent sample in the image, pairs it with the radar backscatter at that sample, and thereby forms the backscatter function: backscatter vs. angle of incidence.

For SP Mountain the pertinent samples were taken on the flanks of the mountain since that is where the topographic sampling was most accurate after the necessary data smoothing, and also where the surface roughness is known to be most homogeneous.

The Fortran computer program to compute the backscatter curve is listed in Appendix D, and the backscatter data is shown in Figure 11.

The scatter in the backscatter data is expected. First, the small-scale roughness is not perfectly homogeneous, since scoria occurs randomaly but statistically equivalently distributed over the flanks, causing a deviation in local backscatter. Unfortunately, the "bible" of radar backscatter by Cosgriff et al.(1960) does not show the scatter or variance in their curves, which we presume to have existed, so we cannot compare the scatter in their data with the scatter found on SP Mountain data. The widest excursions are approximately a factor of two in intensity, or 3 db.

CONSTRUCTION OF PSEUDO-SAR IMAGE

Given the backscatter as shown in Figure 11, a line can be drawn for the average backscatter curve as shown by a dashed line in the Figure. Then for each sample of the topographic data a presumed backscatter value can be computed for the angle of incidence at that sample. Merely assigning a value from the backscatter curve can give a

simulated radar image ("pseudo" SAR image) in ground range.

The pseudo-SAR image in ground range of SP Mountain is shown in Figure 12.

By again relating the ground-range representation to the slant range image--that is, computing the distance to the radar vehicle from each location on the ground--a slant range pseudo image can be constructed. The pseudo-slant range image is shown in Figure 13, and the Fortran program to compute both ground and slant ranges is shown in Appendix E.

SUMMARY

We have developed, illustrated, given the digital Fortran programs for, and plotted a backscatter curve (or rather scatter diagram) from actual SAR data. For this purpose topographic data of the SAR-imaged region was required.

An image was chosen which presented the nearest laboratory-like data available--SP Mountain in Northern Arizona, a right circular cinder cone in which the surface roughness is uniform along its flanks. Continuously varying angles of incidence over a surface with essentially uniform roughness are found in this image.

To assign the backscatter corresponding to the gradient direction at each sample on the image, the slant range representation must be accurately converted to ground range. To achieve this conversion, relief displacement must be rectified, which requires accurate knowledge of the flight

parameters of the radar vehicle. By using control points along a range line, the altitude and groundtrack of the vehicle can be found.

After converting from slant range to ground range, the normal to the local tangent plane at each sample is first found, and then the angle between this normal and the incident radar beam. This latter angle is the angle of incidence. It remains to pair each angle of incidence with the backscatter at each sample point to find the points which will define the backscatter curve.

The above was sketched out, programmed, and achieved. The flanks of SP Mountain were used to test the procedure.

After determining the average backscatter curve, a pseudo image was generated from the topographic data. This image was generated by first finding the angle of incidence from the topographic data and the direction of a radar beam from a presumed location of a radar vehicle. Then the value found from the backscatter curve was assigned to the corresponding angle of incidence. Pseudo-images were obtained and illustrated for both slant and ground ranges.

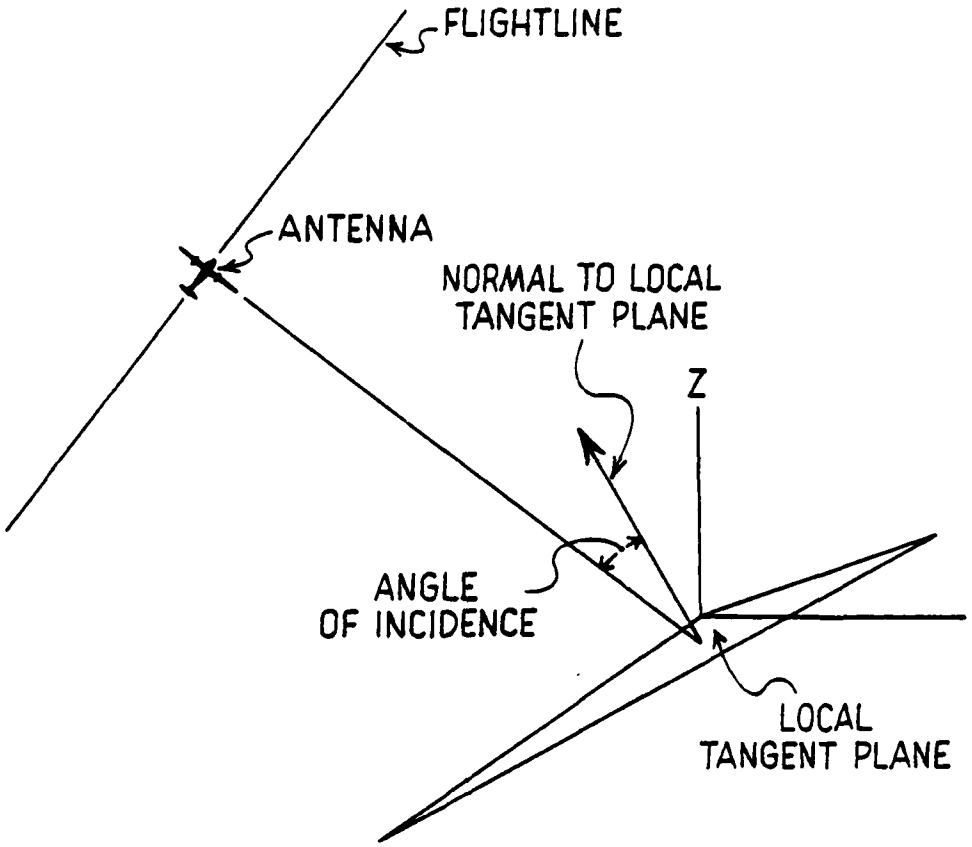

Figure 1. Three-Dimensional Angle of Incidence of Radar Backscatter.

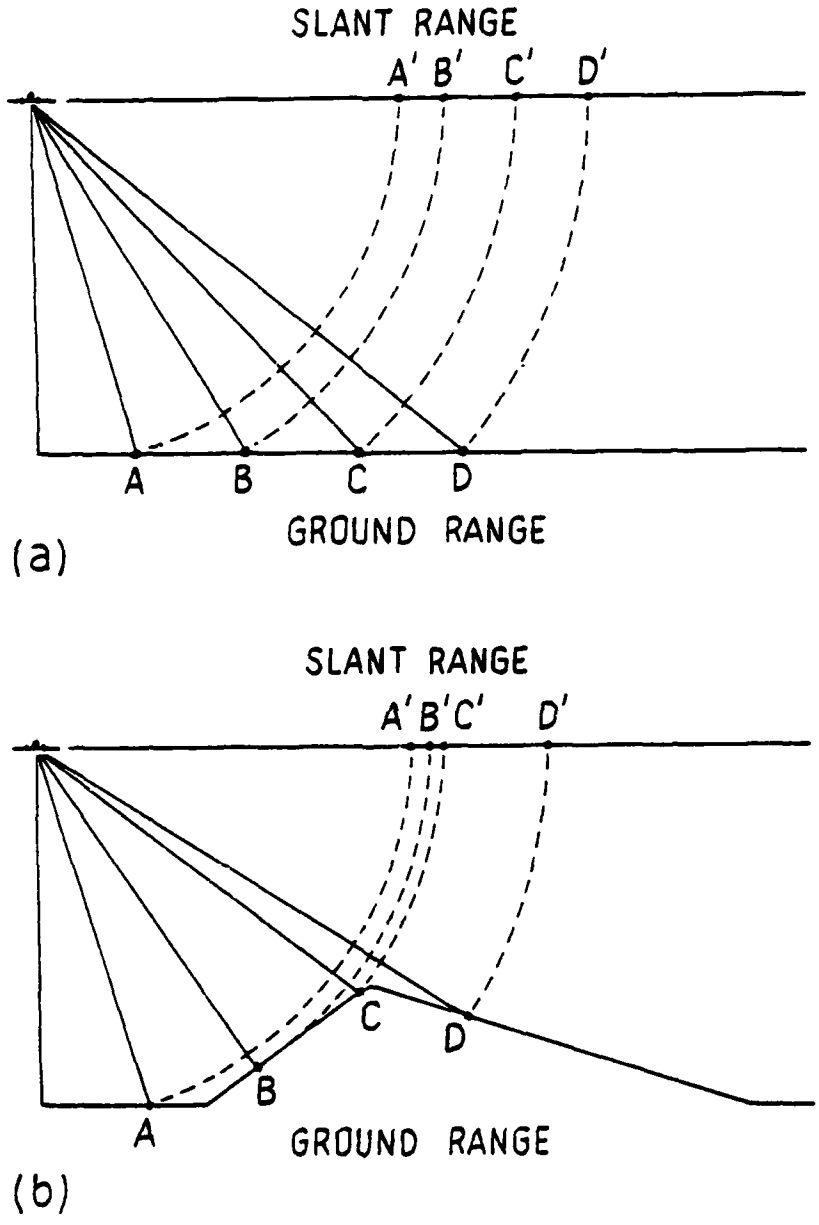

Figure 2. Slant Range Distortion. a) Horizontal Terrain. b) Terrain with Relief Causing Displacement.

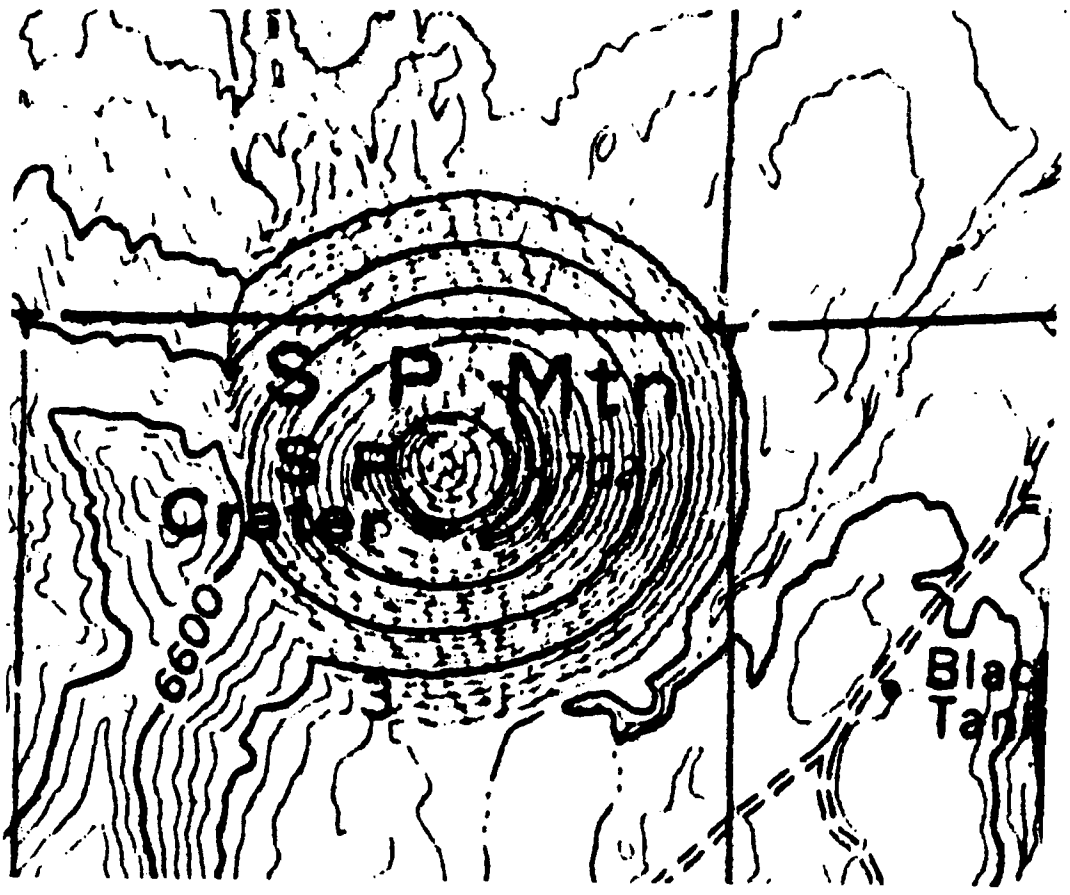

Figure 3. Contour Map of SP Mountain (Scale 1:16,560).

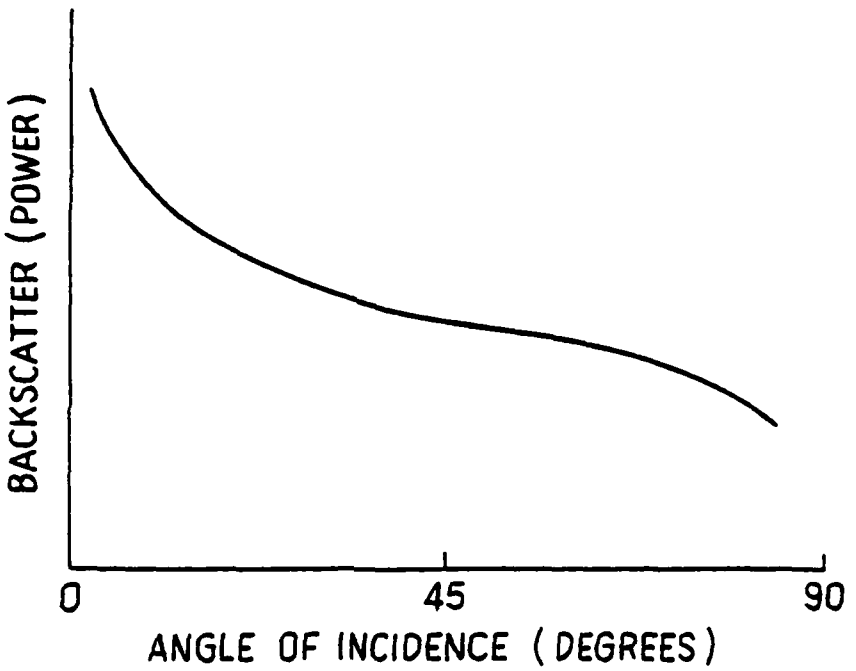

Figure 4. Typical S-Shaped Backscatter Curve.

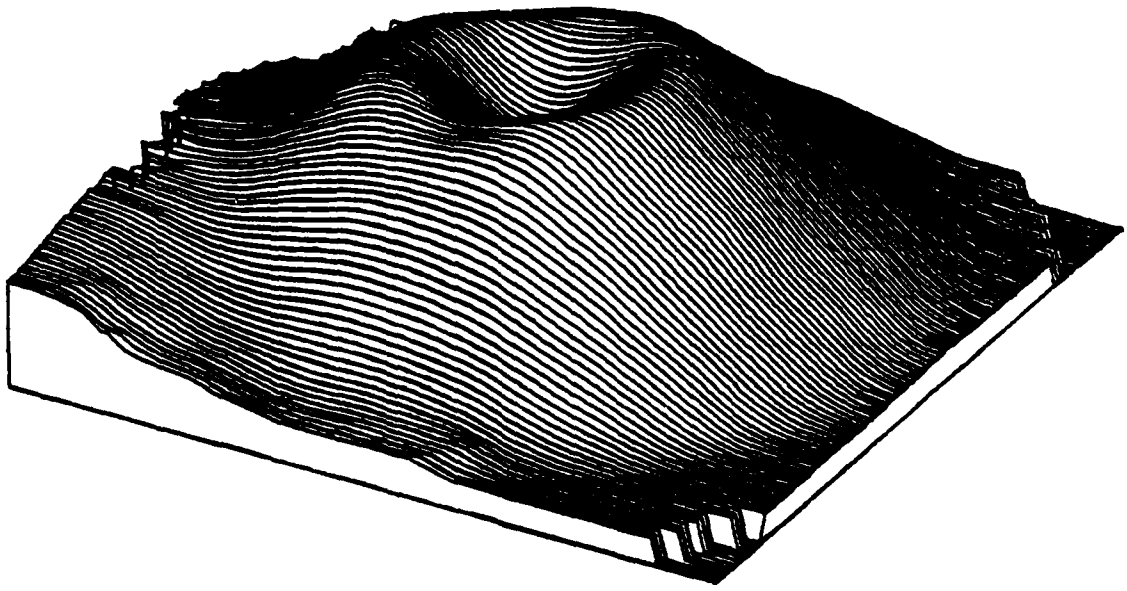

Figure 5. Perspective Plot obtained from Contour Data of SP Mountain (100 x 100 data grid).

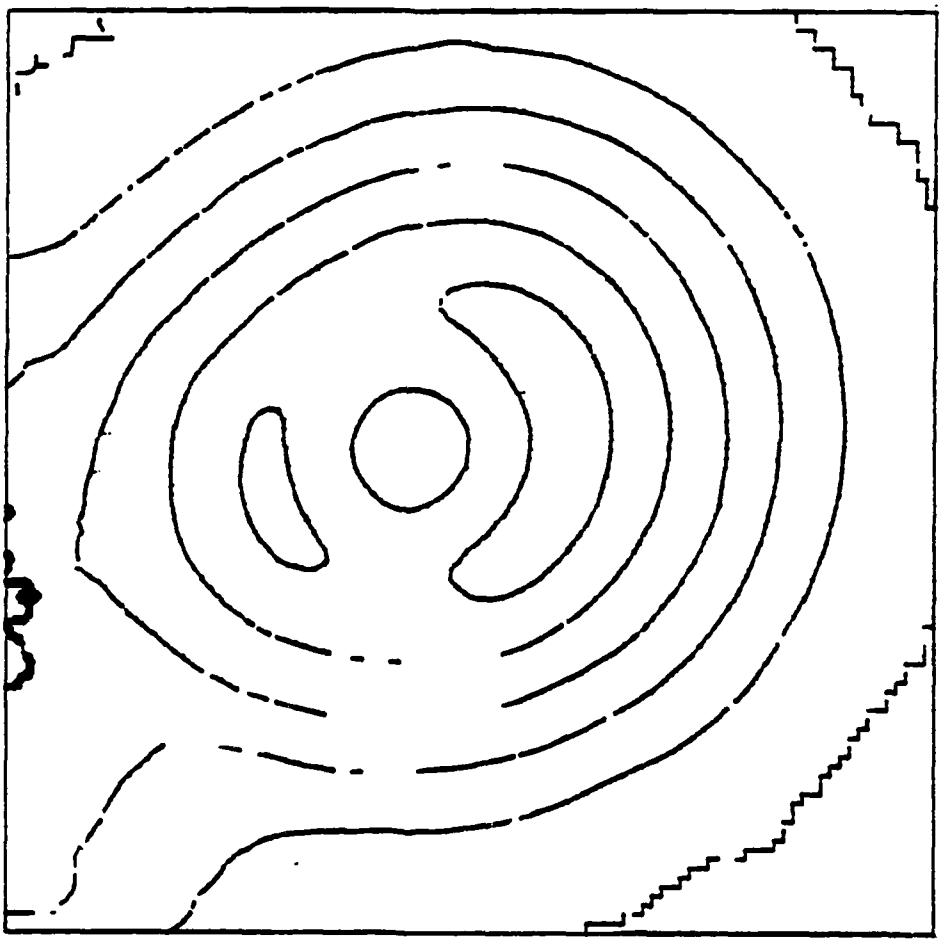

Figure 6. Contour Plot obtained from 100 x 100 Topographic Data Grid of SP Mountain.

Figure 7. SAR Image of SP Mountain in Slant Range (100 x 100 pixels).

Figure 8. SAR Image of SP Mountain in Ground Range (100 x 100 pixels).

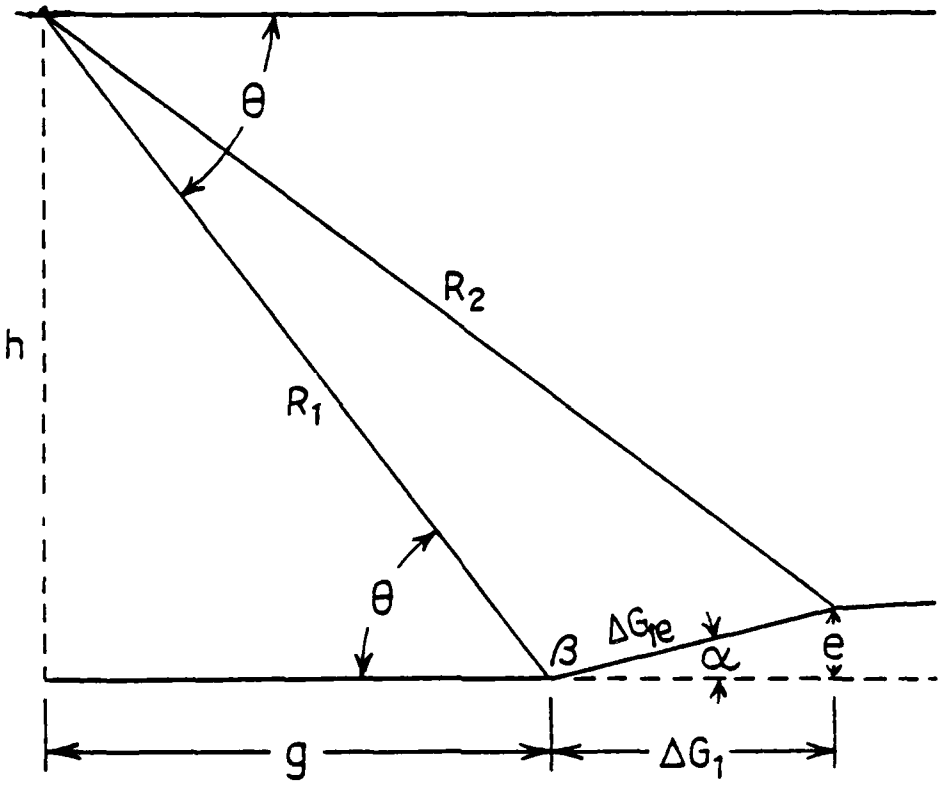

Figure 9. Determination of Aircraft Parameters (Altitude and Groundtrack) when Absolute Slant Range is Known to Two Control Points.

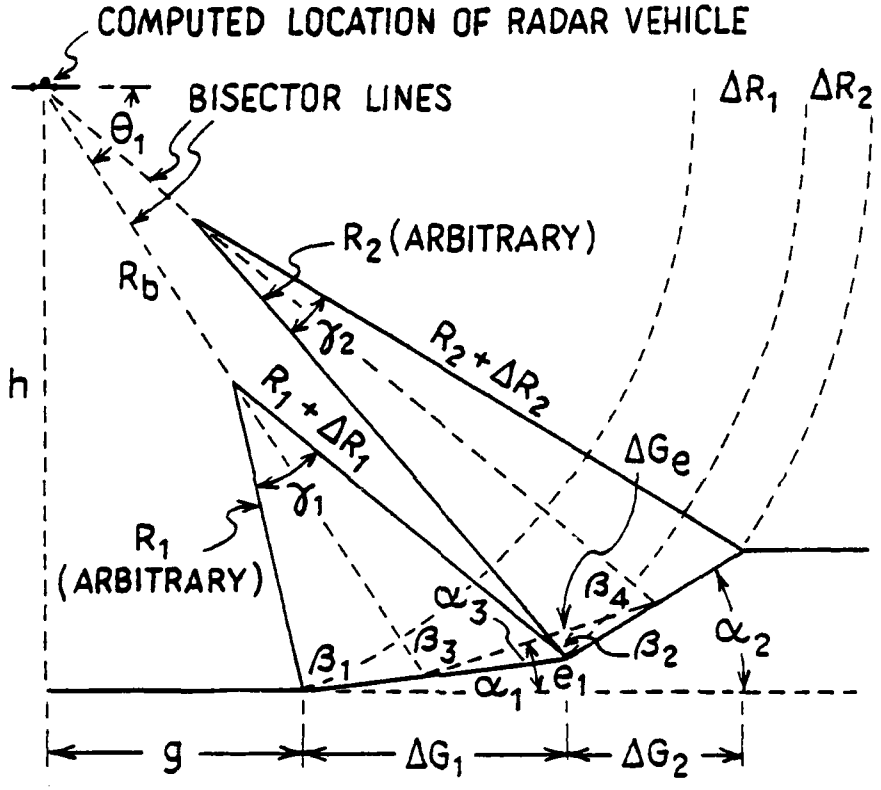

Figure 10. Determination of Aircraft Parameters when only the Differences in Slant Ranges are Known, Using Three Ground Control Points.

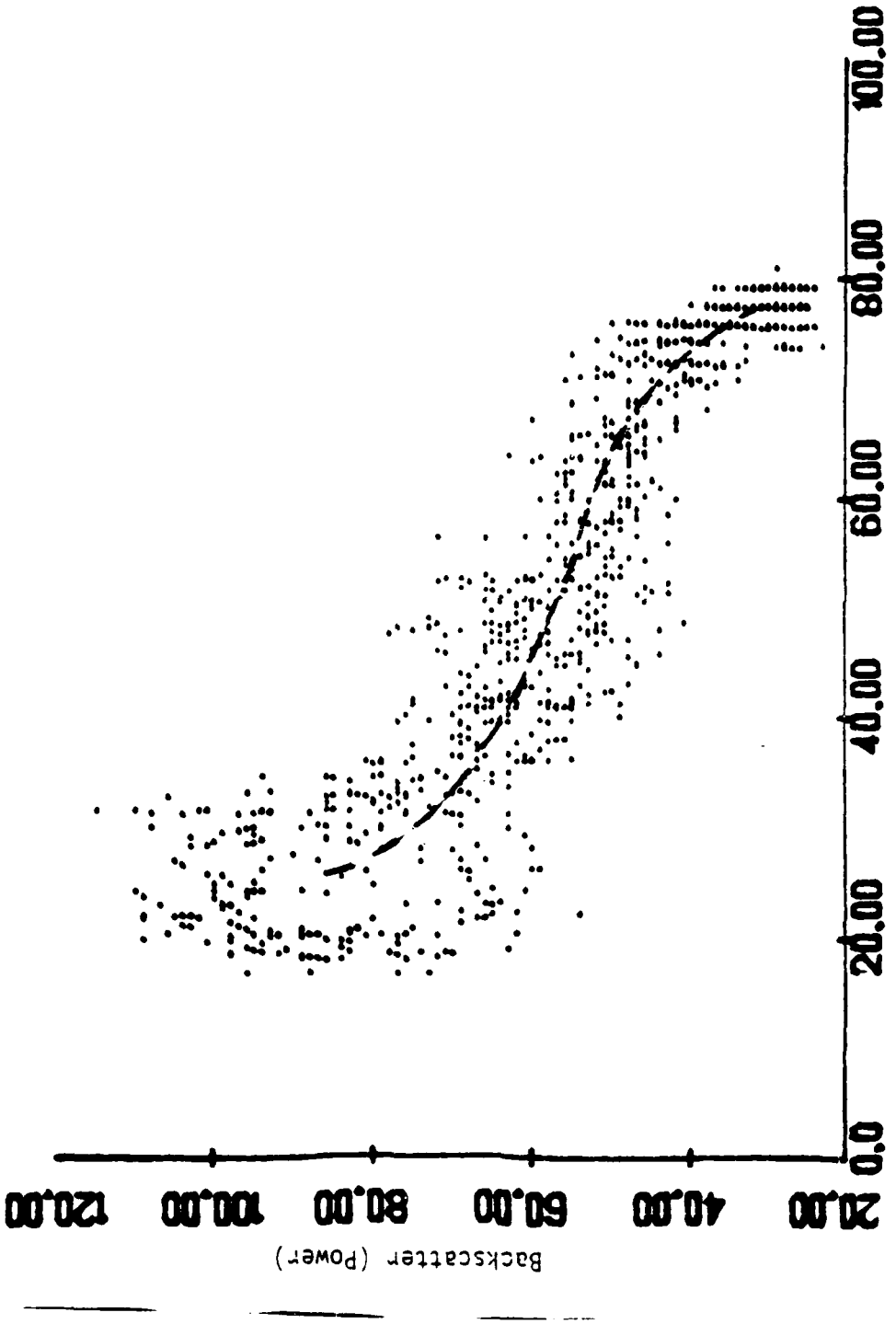

Figure 11. Backscatter DATA (Radar Backscatter vs. Angle of Incidence) Found from Flanks of SP Mountain. Dashed Line is Faired Curve.

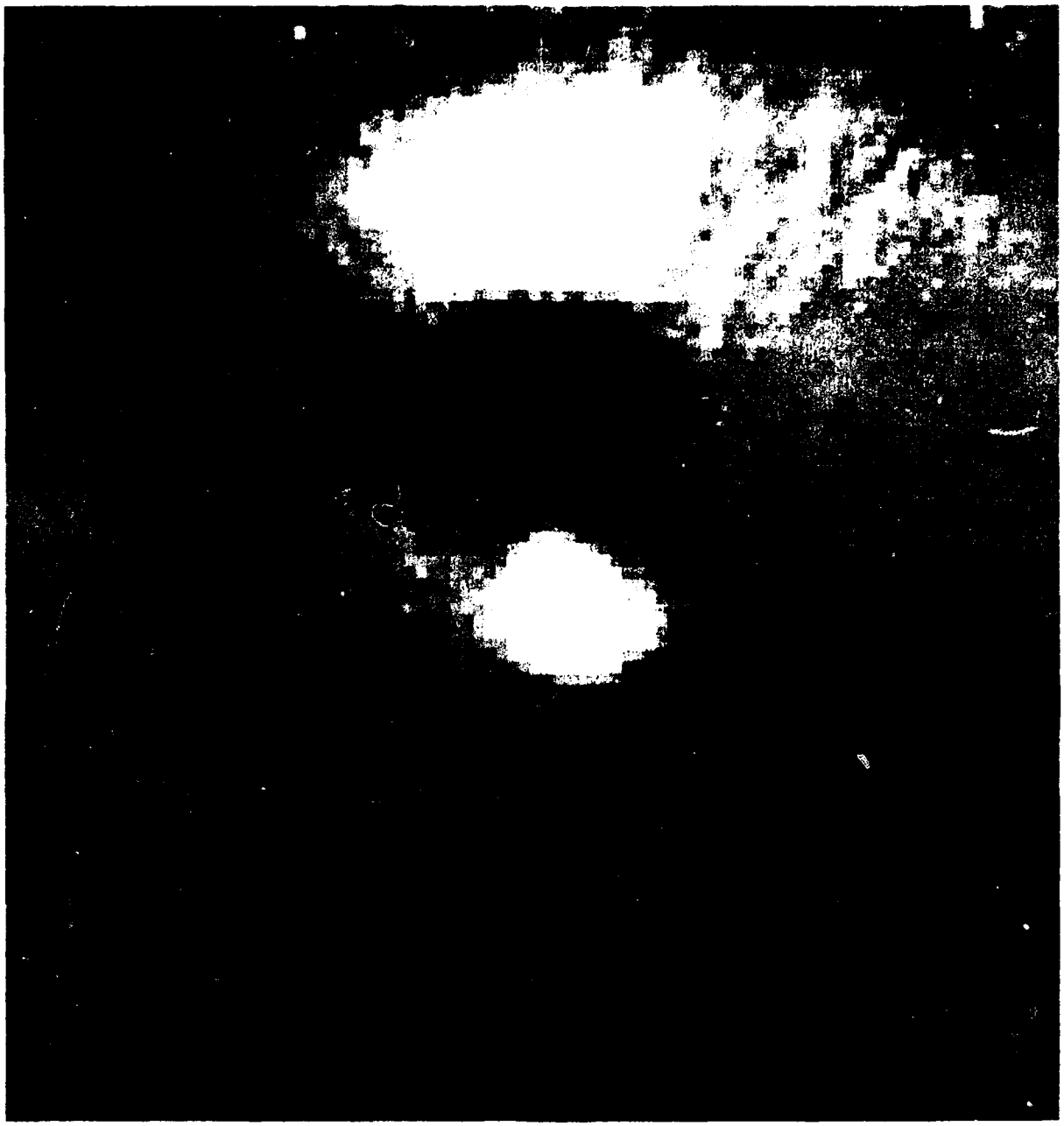

Figure 12. Pseudo-Image of SP Mountain in Ground Range formed from Topographic Data and Backscatter Curve (100 x 100 pixels).

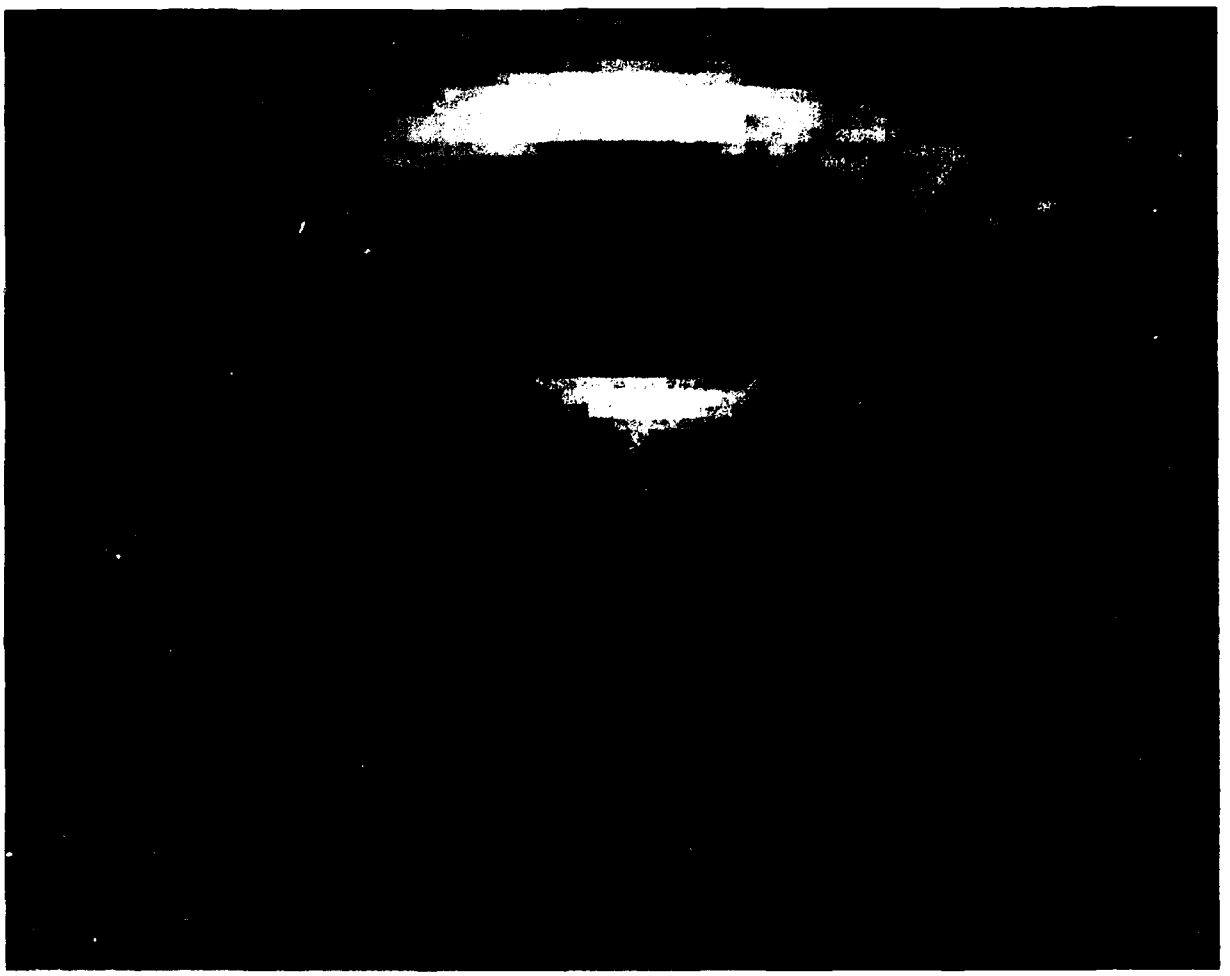

Figure 13. Pseudo-Image of SP Mountain in Slant Range formed from Topographic Data and Backscatter Curve, based on 100 x 100 Pixels in Ground Range.

PART TWO

INTRODUCTION

To contribute to discrimination in SAR imagery between uncultivated, agricultural, suburban, and urban regions, an investigation of the use of the Fourier transform was undertaken. Tests were made to see whether the Fourier transform would be useful as a discriminant in pattern recognition schemes.

The applicability of the Fourier transform to SAR rests on several factors: The processing of SAR requires the formation of a Fourier transform between the signal film or tape and the final image. The transform is achieved both optically and digitally. The Fast Fourier Transform (FFT) is used in real-time processing of SAR data, and therefore is fast enough to use in a real-time classification system. Cultural effects produce pronounced results in SAR imagery--such effects as field boundaries, streets, and dihedral angles of large buildings are accentuated in SAR imagery as compared to photographic or scanning images in the visible and near-visible wavelengths. These effects produce large intensity contrasts in SAR, producing sharp edges and abrupt changes in the image. Also the edges are often aligned.

The Fourier transform, which produces an "image" in the frequency domain, has the following useful attributes:

1) Independence of position of objects
2) Dependence upon orientation
3) Dependence upon spacing of elements
4) Sensitivity to alignments
5) Sensitivity to edges
6) Sometimes simplification of complicated patterns
7) Sometimes elaboration of simple patterns

For this experiment optical and digital two-dimensional Fourier transforms were produced of different types of imagery. These included uncultivated, agricultural, suburban, and urban areas. Optical transforms were primarily for viewing to discover discriminating features which might be used in pattern recognition schemes. Digital transforms were primarily to validate and duplicate the optical transforms, as digital transforms would be required for inclusion in multi-dimensional pattern recognition schemes.

After a discusssion of the two-dimensional Fourier transform, the methods of optical and digital processing will be presented, results from each shown, and conclusions and recommendations drawn. The brief discussions are conceptual, non-mathematical, and heuristic.

THE TWO-DIMENSIONAL FOURIER TRANSFORM

The Fourier transform of a two-dimensional function such as a SAR image produces a transformed "image" in the frequency domain. The mathematical expression is

$$F(\omega_x,\omega_y) = \iint f(x,y)\exp(i\omega(x+y))dxdy$$

Essentially this expression describes the multplication of the function f(x,y) on all horizontal and vertical "lines" in the image by phased sinusoids of all frequencies. If the function along a line in the image contains the same frequency as one of the phased sinusoids, then a non-zero value identified at that frequency will occur in the

integrated value. When all horizontal and vertical "lines" are interrogated in this manner a distribution of values in two-dimensional frequency space (ω_x,ω_y) will be found. This frequency space will indicate the rate of spatial change in the image (x,y) space and in the process reveal the orientation. The frequency space can be thought of as four quadrants, with zero frequency (representing a constant value in the image) at the origin. The distance, in any direction from the origin, indicates the spatial frequency in the image, and the direction indicates the orientation of this spatial frequency. The two-dimensional Fourier transform is always symmetric in the sense of iversion about th origin, the negative frequency being oriented 180° about the oigin from the positive frequency. For this reason only half of the frequency plane is required for display or computation.

Although phase is found with the transform, we are concerned with the magnitude only.

Figure 14 shows the basic relationships of the two-dimensional Fourier transform. Note that frequency is directly proportional to the distance from the origin, and that position of frequency components in the two-dimensional plane indicate the orientation of distributions in the image. Figure 14 illustrates the Fourier transform dependence upon orientation and upon spacing of elements in the image.

The magnitude (but not the phase) of the Fourier

transform is independent of position within the image. Identical distributions with the same orientation all produce identical frequency components in the Fourier transform.

An ensemble of randomly oriented lines will produce a substantially different distribution in the Fourier transform than an ensemble of aligned lines. The energy of the aligned lines will be concentrated, while the energy from the randomly oriented lines will be diffuse in the transform.

From the above it can be seen that sometimes a complicated pattern in an image can be transformed to become a simplified pattern in the Fourier transform. Aligned, but positionally separated distributions produce identical, overlapping patterns in the transforms.

Also, a simple pattern, such as a sharp edge, can produce a more elaborate pattern composed of a series of harmonics. Edges are produced by high frequencies, the more rounded the edges the lower the frequency.

Thus a Fourier transform views an image in different light--in "frequency" space rather than "object" space. Of the seven listed characteristics of the Fourier transform, some may aid in more clearly delineating image differences, or may simplify intricate features.

A final characteristic of the Fourier transform should be mentioned. It is linear--superposition of image characteristics can occur, and the Fourier transform can

delineate the characteristics. An example of this delineation is the transformations of SAR signal film into image film. The signal film is a morass of superimposed zone plates which is uninterpretable in its original form. By exploiting the frequency components and the fact that the Fourier transform is linear, the signal film is metamorphosed into a clear, interpretable image.

THE OPTICAL FOURIER TRANSFORM

It has long been known that a simple optical lens can perform a Fourier transform. The operation is two-dimensional. All that is required is a plane wave of monochromatic light, a replica on which an image is represented in the form of variable light transmission and a simple lens. At the focal point of the lens the two-dimensional Fourier transform of the transmission distribution of the replica is found. Figure 15 illustrates this phenomenon.

The physical operation is straightforward: Diffraction is employed. The higher the spatial frequency, the greater the angle that light will be diffracted. (A coarse grating will diffract light by a small angle, a fine grating by a large angle.) Thus a high frequency will deviate light more than a low frequency, and the relationship between frequency and diffracted light deviation is linear. Therefore, the angle of diffracted light defines the spatial frequency of light transmission within the replica.

A simple lens translates direction of light into position on a plane; in this case the focal plane of the lens. This characteristic gives a lens its imaging capability. A simple, but conceptually valuable, example is that of viewing the stars. The crystalline lens of the eye translates plane waves of light coming from different directins from the stars into a point on the retina--translating light direction into position, the same as a Fourier transforming lens.

The Fourier transform frequency space is optically achieved by the combination of the two steps mentioned above.

The first is the diffraction of light by the spatial distribution in a transparency representing a SAR image. The angle the light deviated by diffraction is directly proportional to the frequency of the spatial distribution in the image, and its transverse direction is governed by the orientation of the diffracting spatial distribution. Therefore the diffracted angle defines the frequency in the transparency.

The second is the action of the lens which focuses each direction of light to a position on a plane. Each position on the plane defines a direction of impinging light on the lens. The energy distribution of light along the focal plane of the lens represents the distribution of light directions impinging on the lens.

Each position on the focal plane thus defines a

direction of impinging light which in turn defines a frequency along the image transparency. Hence the distribution of light in the focal plane of a Fourier transform lens represents the spatial frequency of the transparency.

Such optical processing is extremely efficient. One needs only to place a transparency of an image in a simple optical system to immediately obtain a two-dimensional transform. The efficient, parallel processing achieved with optics is the reason most SAR is processed optically. Two limitations exist, however.

The first, only a small percentage of the energy in the incident light is diffracted, leaving about 96% of the light undiffracted. This forms an intense concentration of light at the center (zero frequency) of the Fourier transform which spreads out into the lower levels of frequency by both the spread function of the focused light and lateral diffusion when photographic film is used. This requires the blocking out of the undiffracted light in obtaining an image.

The second, noise is present, caused by lens imperfections, dust and particles on the lens and in the air, film granularity, and film thickness variations.

The optical setup can be very simple. It consists of a laser source focused upon a pinhole, and one lens to focus the pinhole. The plane of the focus of the pinhole is a close approximation of the Fourier transform. As the scale

of the Fourier transform is proportional to the distance from the replica to the focal plane, the scale can be adjusted as desired. The scale is not controlled by the focal length of the lens, as is the case when using collimated light. It is adjusted by the positions of the lens and the replica. Figure 16 shows the optical setup used for the Fourier transform examples to be shown.

THE DIGITAL FOURIER TRANSFORM

The fast Fourier transform (FFT) is universally used for one- or multi-dimensional digital Fourier transforms. It is computationally efficient, and exists in the program libraries of most computer installations. In the case of SAR images, the input required is a two-dimensional array whose elements represent the image by numerical values at locations corresponding to the indices of the array element. The highest frequency measured is the inverse of twice the sampling interval (the Nyquist frequency) and the resolution is the Nyquist frequency divided by the total number of sample points.

The FFT is fast enough that a transform can be obtained in real time; in fact, as noted previously, it is fast enough to process SAR data from its recorded form to image form in real time.

The output is, of course, in digital form, and can therefore be used drectly in pattern recognition schemes.

For the examples in this report samples of the image

were recorded in a 128 x 128 array of an image approximately 3.2 x 3.2 km, giving a sample interval of approximately 25 m.

OPTICALLY PROCESSED EXAMPLES

An optical setup similar to that of Figure 16 was used to obtain a series of optical Fourier transforms of various types of terrain. A 12-inch focal length lens was used, where the distance from the pinhole to the lens was 0.5 m, from the lens to the image of the pinhole was 4.67 m, and the replica (image transparency) was placed a distance 3.5 m from the pinhole. A photographic film is placed in the plane of the focused pinhole to record the transform. An additional lens is then inserted to record the actual image with displacement of the recording film, so that the image is then recorded on the same film as the transform.

To reduce the effect of the aperture the square image transparency is "apodized" by inserting a circular aperture to produce diffraction that is diffuse as opposed to concentrated with a square or straight-sided aperture.

Since the undiffracted light is so intense, and focuses at zero frequency of the transform, an opaque shield must be inserted to be able to record the light by low spatial frequencies. These are the dark portions of the transforms in Figures 17 to 19. These shielded portions blot out half of the transform plus a small region around zero frequency. As stated before, the magnitude of the two-dimensional

transform is symmetric by inversion around its origin; therefore all information is contained in only two of four quadrants.

The radar images used in this report were supplied by ERIM, and were obtained with their X-L system. The images were all optically processed.

Figure 17 shows the SAR image and Fourier transform of uncultivated land in western North Carolina. It was obtained with X-Band (3 cm) horizontally transmitted and horizontally recieved polarization (HH) flown in April, 1974. The terrain is composed of low lying hills not rigidly oriented in one direction. There are no sharp edges in the image, therefore no high frequencies. As the orientation is not restricted, diffraction occurs almost equally in all directions. The energy distribution in the transform is therefore relatively evenly distributed, and of relatively low frequency.

Figure 18 shows the SAR image and OFT of agricultural land in Michigan. This image also is X-Band HH, obtained in September, 1979. Note the sharp boundaries of the agricultural fields which produce relatively sharp lines in the image. The bright boundary lines are caused by brush and other vegetation along fence lines of the fields. Other than these sharp lines there is essentially no spatial frequency variation in the image. These boundary lines diffract light perpendicular to their directions, which in this case, with square fields, are at right angles. The

diffraction also is at right angles, manifesting itself as two perpendicular broken lines pointing at the center of the transform, which, of course, is blocked off. Although the field boundary lines are located at many different places on the image, they all diffract to the same line, since the Fourier transform energy distribution is independent of position in the transformed image. The series of frequencies along the lines in the OFT are the harmonics of the sharp edges found in the image.

Figure 19 shows the SAR image and OFT of a suburban area, Ypsilanti, Michigan, an X-Band HH image obtained in September, 1979. Here the sharp edges are due to streets rather than field boundaries. Again the diffraction will be prpendicular to the direction of the lines and will be positionally independent. So lines, formed of harmonics, will appear in the OFT, the strength of which are based upon the number of lines of a particular orientation as well as their sharpness. Here the OFT lines are a little more intense that those from the agricultural fields, and the harmonics are more closely spaced.

DIGITALLY PROCESSED EXAMPLES

The digitally Fourier transformed data was processed from SAR data represented on a 128 x 128 array. Available data were in an optically processed form, making it necessary to digitize directly from this image. The data were digitized directly from an image transparency using an Optronics 100 instrument. The original digitization was 512

x 512 samples over an image representing approximately a 3.2 x 3.2 km area, giving a sampling interval of approximately 6.25 m.

The data were first reduced to a 128 x 128 format by 4 x 4 median filtering. Median rather than averaging filtering was performed because this type of filtering tends to retain sharp edges much more so than averaging (weighted or otherwise).

As the aperture effect occurs with digital as well as optical transforming, the square image is then digitally apodized by approximating a circular aperture whose perimeter touches the midpoints of the edges of the square. Values of all elements between the circle and the square are set to zero.

To eliminate zero frequency first differencing was also employed. Untreated digital data often produces large values at and near zero frequency. First differencing (see Jenkins and Watts, 1968) produces a gradual rolloff from a low frequency to zero frequency.

The three operations of median filtering, apodizing, and first differencing are performed in the Fortran program listed in Appendix F.

Figure 20 shows the two-dimensional FFT of the uncultivated area shown in Figure 17. The Figure is of contour values at 0.5 and 0.95 when the maximum is normalized at 1.0. The energy in the transform is approximately equally distributed around zero frequency.

Only half the Fourier transform is shown.

Figure 21 shows the two-dimensional FFT of an agricultural region nearby, but not identical to the area used for the OFT transform shown in Figure 18. Again two broken lines perpendicular to the field boundaries and pointed at the lcation of zero frequency are shown. The lines representing the harmonics of the sharp edges of the field boundaries are again evident.

Figure 22 shows the two-dimensional FFT of an urban area nearby but not identical to that shown in Figure 19. Here the transform does not reflect the street boundaries. Its results are similar to that of the uncultivated area of Figure 7. This similarity is thought to be due to sampling problems rather than intrinsic to the image.

DISCUSSION

The Fourier transform as a discriminant in pattern recognition was looked into by taking many OFT's of different types of terrain. These were examined for differences between types of terrain. The most striking difference was between uncultivated terrain and terrain in which man-made cultural features are present, the latter being agricultural, suburban and urban environments. Such man-made features as field boundaries, roads, streets, and buildings tend to be built with straight lines as well as to exhibit relatively sharp discontinuities.

A straight contrasty line on an image transparency will

cause light to diffract perpendicularly into a narrow line composed of relatively high frequency harmonics. Parallel lines will cause all the diffraction to be superimposed on one line in the OFT, making a distinctive pattern. This pattern differs markedly from patterns formed from images of uncultivated areas. The OFT's shown in Figures 17 and 18 exhibit this contrast. In Figure 17 the energy in the OFT is fairly uniformly distributed about the origin. In marked contrast the energy shown in Figure 18 is mostly confined to two lines. These lines are perpendicular to the field boundaries in agricultural terrain.

The contrast between the FFT in Figure 17 and those from cultured areas was confirmed by OFT's of other images, and is clearly explained by diffraction theory. The contrast is definite in the Fourier transform, and could be used as an input in a pattern recognition scheme.

The OFT's were obtained for visual comparison. Their use in an actual system would be questionable, because they are obtained from processed film made after the data gathering flight, they contain noise, and have approximately 96% of their intensity at and near zero frequency, which must be blocked out. Even with an output of a light sensitive array or video conversion, the delay, noise, and problems with undiffracted light would negate the practical use of OFT's for discrimination purposes.

FFT's appear much more practicl for discrimination purposes. They are fast, noise-free except for sampling

problems, and their output is digital for direct input into a pattern recognition scheme. Transparent SAR images on film were digitized, resampled with median filtering, apodized, and first-differenced. Digitized at 6.25 m sampling intervals, the images were resampled to 25 m intervals before taking a 128 x 128 two-dimensioanl FFT.

Although the OFT's were described in terms of diffraction of light for visualizing purposes, precisely the same operations occur on the image by the FFT as with the OFT. Sharp, straight lines cause the same pattern in the FFT as in the OFT. This is seen on the FFT's in Figures 20 and 21, which correspond to the OFT's in Figures 17 and 18. The natural, uncultivated area shows relatively low frequency, uniformly distributed energy, and the agricultural areas show concentrated line-like higher frequency energy in both the FFT and the OFT.

The urban FFT shown in Figure 22 looks more like the uncultivated area. This is undoubtedly because of the sampling. The frequencies are so high in both directions that the resampling at 25 meters loses the sharp edges. This illustrates that care must be taken in digitizing and sampling when using the FFT.

This preliminary work indicates that the Fourier transform can be used to discriminate between cultural and non-cultural regions. A simple algorithm can distinquish between the patterns of Figure 20 and 21, so that the result could be an input to a pattern recognition scheme. It has

not been demonstrated here, however, that intracultural types of terrain can be distinquished by the Fourier transform.

The word preliminary is used because a much more extensive testing and statistical evaluation is required. The subtleties were not reached in the time of this investigation. Many problems remain in evaluating the FFT for this purpose:

1) Find and evaluate imagery with gradations of agriculture. For example, what is the FFT when one or a few farms are located in an otherwise uncultivated area.

2) Evaluate FFT's of different kinds of uncultivated areas, such as mountains, deserts, swamps, etc. Although no sharp straight edges would be expected, directional trends might tend to concentrate energy in the FFT.

3) Find the optimal scale and tradeoff between area of image and sampling interval of the FFT. For example, would sampling by 256 x 256 of the same area, or 128 x 128 of 1/4 the area be adequate for urban images.

4) Attempt to use directly recorded digital data. The data used here had been converted three times by optical means--recorded on signal film, processed to image film, and converted to digital form. Only these data were available.

5) Statistically evaluate a significant number of transforms in each category. Here a pattern was observed, and then more OFT's were obtained to see if they were similar.

6) Develop the algorithms to discriminate at least between cultural and uncultivated area. Although the approach is quite clear, time and priorities prevented this development.

7) Incorporate into a pattern recognition scheme and evaluate the benefit of the FFT. Although planned, this was not achieved.

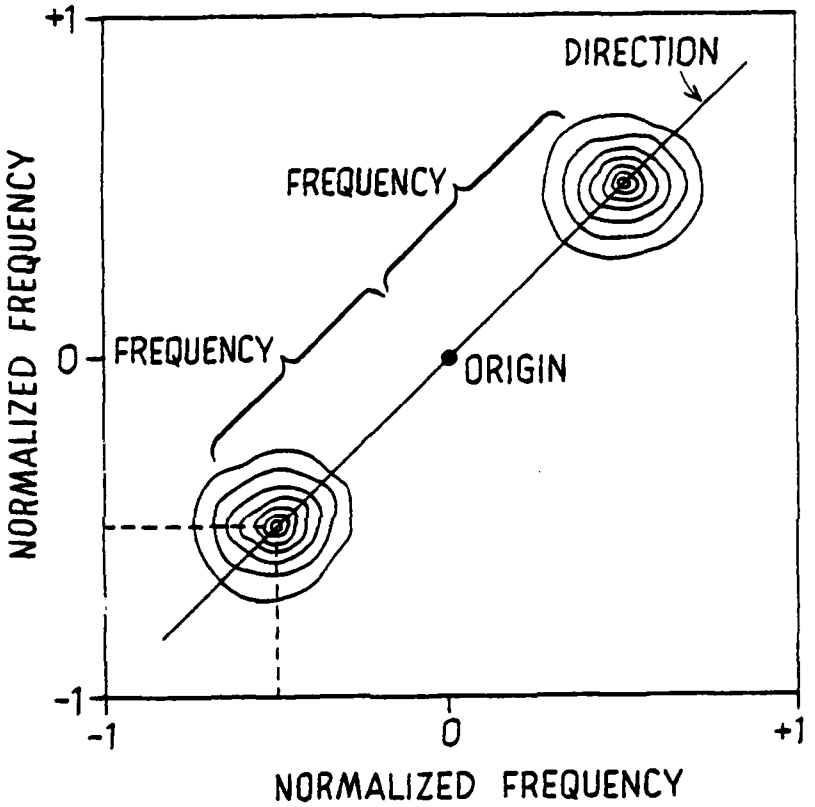

Figure 14. Schematic Representation of Two-Dimensional Fourier Transform. Four Quadrants Shown. Symmetric in Sense of Inversion about the Origin.

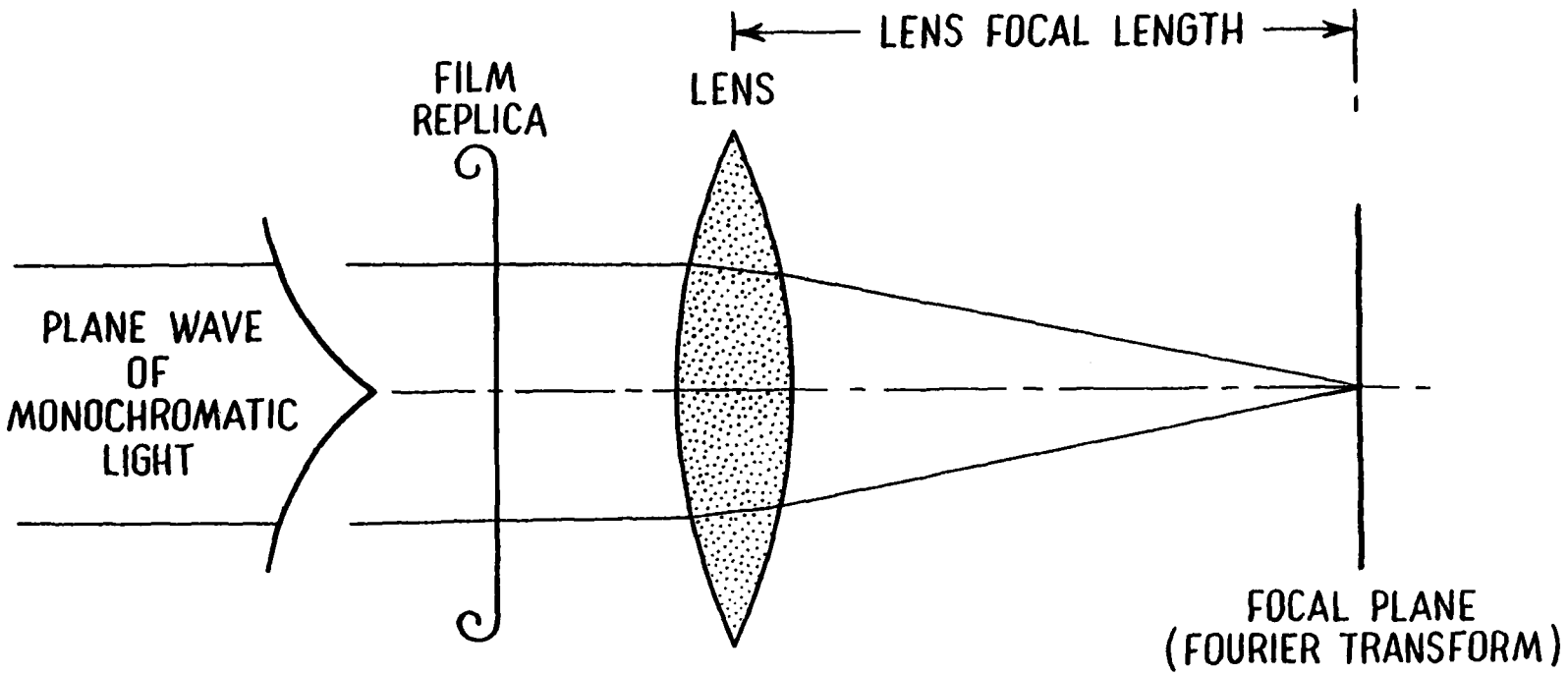

Figure 15. Side View of Fraunhofer Diffraction Optical System to Produce Optical Fourier Transform (OFT) of Light Transmission Characteristics of Replica. Scale of OFT is Proportional to Lens Focal Length.

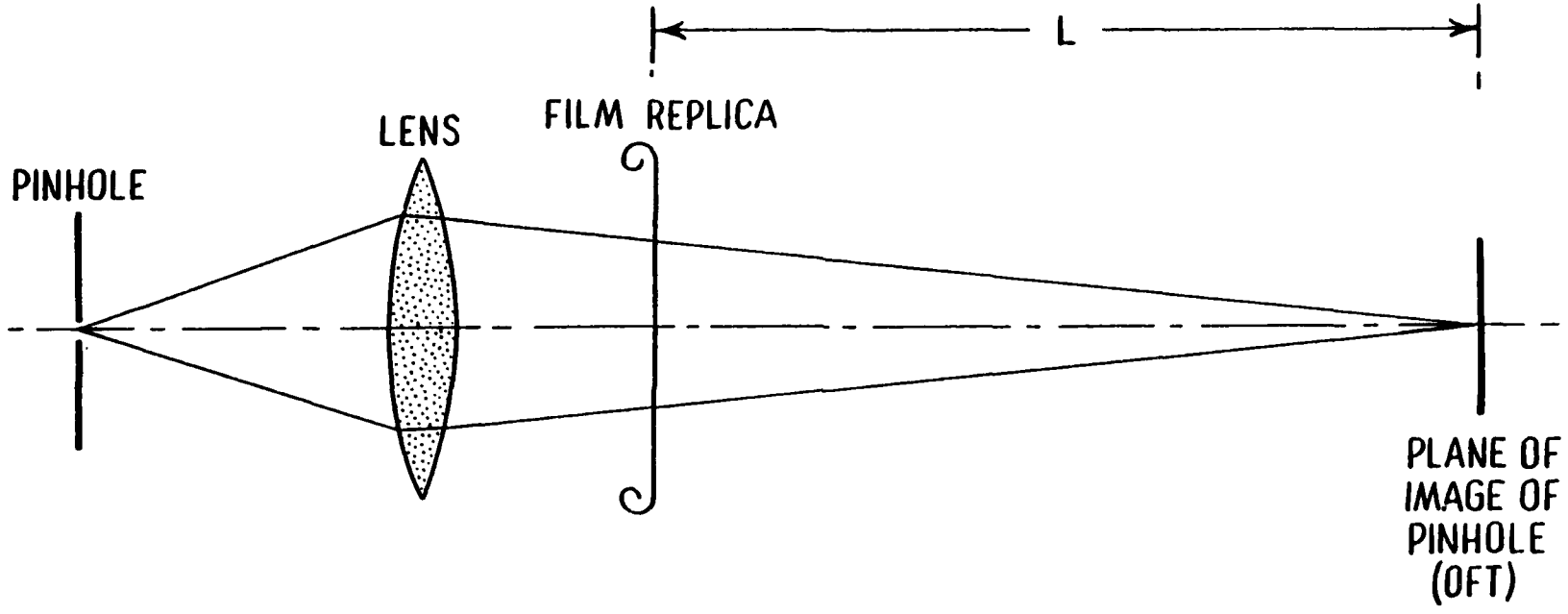

Figure 16. Side View of Simple Optical System to Achieve Close Approximation of OFT of Light Transmission Characteristics of Replica. Scale of OFT is Proportional to length L.

Figure 17. SAR Image and Optical Fourier Transform of Uncultivated Area.

Figure 18. SAR Image and OFT of Agricultural Area.

Figure 19. SAR Image and OFT of Urban Area.

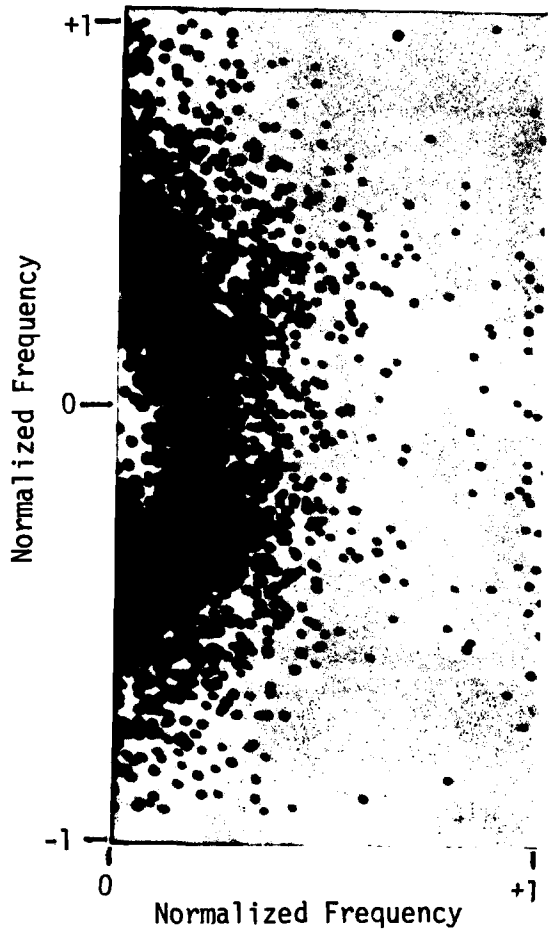

Figure 20. Two-Dimensional FFT of SAR Image of Uncultivated Area. Two Right Quadrants. Contoured Data.

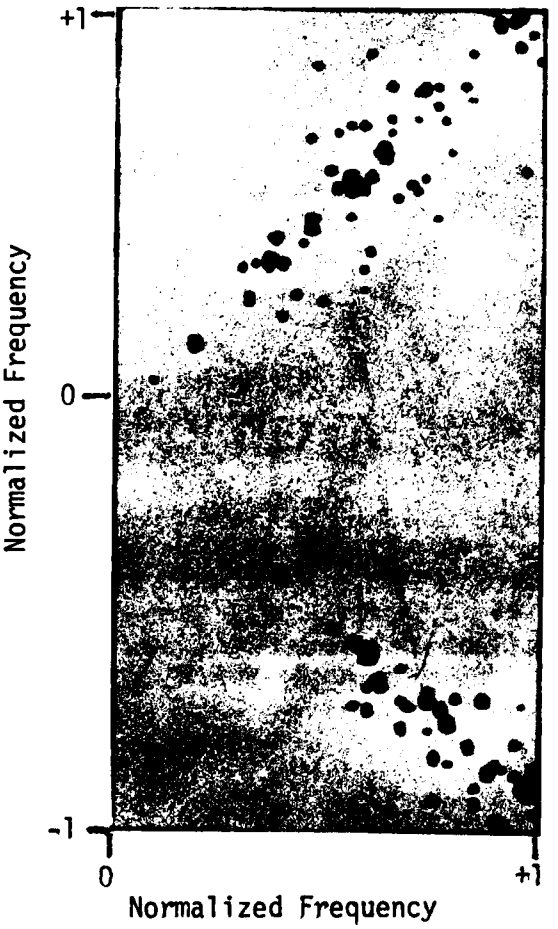

Figure 21. Two-Dimensional FFT of SAR Image of Agricultural Area. Two Right Quadrants. Contoured Data.

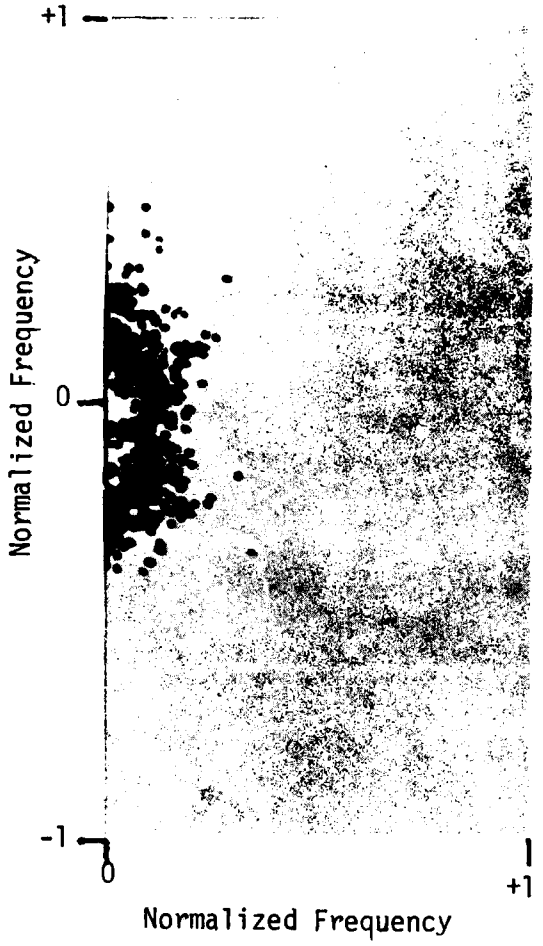

Figure 22. Two-Dimensional FFT of SAR Image of Urban Area. Two Right Quadrants. Contoured Data.

REFERENCES

Ford, J.P., J.B. Cimino, and C. Elachi, Space Shuttle Columbia Views the World with Imaging Radar: the SIR-A Experiment, Jet Propulsion Laboratory Publication 82-95, January, 1983.

Jenkins, G.M., and D.G. Watts, Spectral Analysis and its Applications, Holden-Day, San Francisco, 1969.

Rawson, R.F., R.E. Hamilton, C.L. Liskow, A.R. Dias, and P.L. Jackson, SP Mountain Data Analysis, ERIM Final Report 148000-F to NASA, September, 1981.

Schaber, G.G., C. Elachi, and T.G. Farr, Remote Sensing Data of SP Mountain and SP Lava Flow in North-Central Arizona, Remote Sensing of the Environment 9:149-170 (1980).

APPENDIX A

FORTRAN PROGRAM
TO FILL IN MATRIX FROM
RANDOMLY SAMPLED
ELEVATION DATA

```
C         Take randomly spaced contour data and put in
C            uniformly spaced form
C         Special program for data digitized at
C            0.001 IN FROM 1:62500 scale map
C         1000 x 1000 sample points (5.20823 ft/sample)
C            sample) corresponds to a total of
C             1587.7 meters in each direction
C         For a 12 meter sample interval we need.
C             100 samples.
C
      SUBROUTINE GRID(IX,IY,IZ,IZ1,IZ2)
      DIMENSION IX(1200),IY(1200),IZ(1200),
     1IZ1)192,192),IZ2(192,192)
C
         IX  is  horizontal location on map
         IY  is  vertical location on map
         IZ  is  elevation located by ix and iy
         IZ1  is  2-dim array for nearest
            neighbors
         IZ2  is  2-dim array filled in by
C             averaging IZ1
C        Zero out arrays for data
      DO 20 J = 1,160
      DO 20 I = 1,160
      IZ1(I,J) = 0
      IZ2(I,J) = 0
   20 CONTINUE
      ITIME = 0
C
C        Bring coordinates to origin by subracting minima,
C            minima
C            and change range from 771 to 100,
C            (ratio = 0.13228)
C            and add 30 so that data is not at edge.
C            of array
          Place data in array.
      FACT = 0.13228
      DO 30 I = 1,1171
      IX(I) = (IX(I)-26669)*FACT + 31.5
      IY(I) = (IY(I)-7304)*FACT + 31.5
      IF (IX(I).GT.130) GOTO 30
      IF(IY(I).GE.1) IZ1(IX(I),IY(I)) = IZ(I)
   30 CONTINUE
   31 CONTINUE
C
C        Examine block by going through 100 x 100
C            array points
      DO 40 J11 = 31,130
      DO 40 I1 = 31,130
      J1 = 161-J11
      ICOUNT=0
      ISUM = 0
C        Go through successively larger blocks
C            around array point
```

```
      DO 50 K = 1,4
      K1 = 2*K+1
      K1STEP = K1 - 1
      DO 60 J2 = 1,K1,K1STEP
      DO 60 I2 = 1,K1
      I3 = I1 - K - 1 + I2
      J3 = J1 - K - 1 + J2
      IF(IZ1(I3,J3).EQ.0) GOTO 60
      ISUM = ISUM + IZ1(I3,J3)
      ICOUNT=ICOUNT+1
   60 CONTINUE
C
      K1 = K1 - 1
      DO 70 J4=2,K1STEP
      DO 70 I4 = 1,K1,K1STEP
      I5 = I1 - K - 1 + I4
      J5 = J1 - K - 1 + J4
      IF(IZ1(I5,J5).EQ.0) GOTO 70
      ISUM = ISUM + IZ1(I5,J5)
      ICOUNT=ICOUNT+1
   70 CONTINUE
C
   50 CONTINUE
      IF(IZ1(I1,J1).NE.0) GOTO 41
      IF(ICOUNT.EQ.0) GOTO 40
      IZ2(I1,J1) = ISUM/ICOUNT
      GOTO 40
   41 IZ2(I1,J1) = (ISUM +IZ1(I1,J1))/(ICOUNT+1)
   40 CONTINUE
      IF(ITIME.EQ.1) GOTO 42
      DO 80 J=1,160
      DO 80 I=1,160
   80 IZ1(I,J) = IZ2(I,J)
      ITIME=ITIME+1
      IF(ITIME.EQ.1) GOTO 31
      RETURN
      END
```

APPENDIX B

FORTRAN PROGRAM
TO CONVERT SLANT RANGE SAR IMAGERY WITH RELIEF DISPLACEMENT
TO GROUND RANGE

```
C          Subroutine slagro, which converts slant
c             range data to ground range using
C             topographic data
C
      SUBROUTINE SLAGRO(ISR,IGR,IELEV,INSRS,DELTA,
     1ALT,GRIS,RIS,LIM)
      DIMENSION IGR(100,100),ISR(100,100),
     1INSRS(100,100),IELEV(100,100)
C
C         ISR  is  slant range data
C         IGR  IS  ground range data (to be found)
C         IELEV  is  topographic data
C         INSRS  is  slant range index for ground
C             range
C         DELTA is  slant range sampling interval
C         ALT  is  SAR vehicle altitude
C         GRIS  is  ground range to inside edge of
C             swath
C         SRIS  is  slant range to inside edge of
C             swath
C         LIM  is  number of x,y elements in array
C
      DO 10 I1 = 1;LIM
      ARG1=(GRIS+(I1-1)*DELTA)**2
      ARG2 = (ALT-IELEV(I1,K))**2
      SRDIST = SQRT(ARG1+ARG2)
      I2 = 1.5 + (SRDIST-SRIS)/DELTA
      IF(I2.GT.LIM.OR.I2.LT.1) GOTO 10
      IRDIST = SRDIST+1
      I2 = 1.5 + (IRDIST-SRIS)/DELTA
      DRDIST = SRDIST-IRDIST+1
      IGR(I1,K) = ISR(I2,K-3)+DRDIST*
     1(ISR(I2+1,K-3)-ISR(I2,k-3))
      INSRS(I1,K) = I2
   10 CONTINUE
      RETURN
      END
```

APPENDIX C

THREE FORTRAN PROGRAMS TO DETERMINE RADAR VEHICLE ALTITUDE AND GROUNDTRACK

```
C        Find SAR vehicle parameters when the
C             range to two separate points on a
C             rangeline, and the ground locations
C           and elevations of these points are known.
C
      SUBROUTINE PARAM1(R1,R2,E1,E2,G1,G2,H,G)
C
C        R1  is  range to closer point
C        R2  is  range to farther point
C        E1  is  elevation at closer point
C        E2  is  elevation at farther point
C        G1  is  horizontal distance of closer
C           point from some reference
C        G2  is  horizontal distance of farther
C           point from the same reference.
C        DELGT  is  distance along terrain (up or
C           down slope) between control points.
C        H  is  Vehicle altitude above elevation
C           of closer control point.
C        G  is  Distance from groundtrack to
C           closer control point
C
      DELE  =  E2 - E1
      DELG = G2 - G1
      ALPHA = ARTAN(DELE/DELG)
      DELGT = DELG/COS(ALPHA)
      BETA = ARCOS(DELGT**2 + R1**2 - R2**2)
     1/(2.*R1*DELGT)
      THETA = 3.14159 - BETA - ALPHA
      H = R1*SIN(THETA)
      G = R1*COS(THETA)
      RETURN
      END
C        Find SAR vehicle parameters when only
C             difference in range between, and the
C           the ground locations and elevations of,
C           three control points are known.
C
      SUBROUTINE PARAM2(DELR12,DELR23,E1,E2,E3,
     1G1,G2,G3,RARB,H,G)
C
C        DELR12  is  difference in range between
C             control points 1 and 2
C        DELR23  is  difference in range between
C             control points 2 and 3
C        E1  is  elevation at control point 1
C        E2  is  elevation at control point 2
C        E3  is  elevation at control point 3
C        G1  is  horizontal distance from
C           reference to point 1
C        G2  is  same from point 2
C        G3  is  same from point 3
C        RARB  is  arbitrary (guessed) range
C        H  is  altitude above E1
```

```
C         G  is  grountrack
C
C         Get bisector lines:
      DELG12 = G2 - G1
      DELG23 = G3 - G2
      DELE12 = E2 - E1
      DELE23 = E3 - E2
      ALPHA1 = ARTAN(DELE12/DELG12)
      ALPHA2 = ARTAN (DELE23/DELG23)
      DELGT1 = DELG12/COS(ALPHA1)
      R1 = RARB
      R2 = RARB + DELR12
C
      DO 10 I = 1,2
      DO 20 J = 1,2
      BETA = ARCOS(DELGT1**2 + R1**2 - R2**2)/
     1(2.*R1*DELGT1)
      BUF = 3.14159 - BETA - ALPHA
      IF (J.EQ.1.AND.I.EQ.1) THETA1 = BUF
      IF (J.EQ.2.AND.I.EQ.1) THETA2 = BUF
      IF(J.EQ.1.AND.I.EQ.2) THETA3 = BUF
      IF (J.EQ.2.AND.I.EQ.2) THETA4 = BUF
      BUF = R1
      R1 = R2
      R2 = BUF
   20 CONTINUE
      DELGT1 = DELG23/COS(ALPHA2)
      R1 = RARB
      R2 = RARB + DELR23
   10 CONTINUE
C
      BISEC1 = ABS((THETA1-THETA2)/2.)
      BISEC2 = ABS((THETA3 - THETA4)/2.)
      G12 = (G1 + G2)/2.
      G23 = (G2 + G3)/2.
      E12 = (E2 - E3)/2.
      E23 = (E3 - E2)/2.
      GE12 = E12/TAN(BISEC1)
      GE23 = E23/TAN(BISEC2)
C
C         We now have one side and two angles of
C            a triangle.
      SIDE = ABS(GE23 - GE12)
      ANGLE1 = 3.14159 - BISEC1
      ANGLE2 = BISEC2
      ANGLE3 = 3.14159 - ANGLE1 - ANGLE2
C
C         Using law of sines:
      R1 = SIDE*SIN(ANGLE2)/SIN(ANGLE3)
      H = R1*SIN(BISEC1)
      G = R1*COS(BISEC1)
      RETURN
      END
```

```
C        Using one range line, vary the
C           altitude to obtain a set of ground
C           ranges for visual comparison with map.
C
C     SUBROUTINE ALTVAR(ISR,IGR,IELEV,INSRS,SRIS,ALT,GRIS)
      DIMENSION ISR(100),IGR(100),IELEV(100),INSRS(100)
C
C        ISR  is  one range line of SAR data
C        IGR  is  the range line in ground range(to be C
found)
C        IELEV  is  one raster lin of topographic data
C        INSR  is  list of slant range sample numbers
C           corresponding ground range samples
C        SRIS  is  slant range to inside of swath (constant)
C        ALT  is  altitude of vehicle (iterated)
C        GRIS  is  ground range to inside edge of swath
C
      SRIS = 5582.4
      ALT = 5600.
      DELTA = 12.
      LIM = 100
      DO 30 K = 1,100
   30 IELEV(K) = IELEV(K)/3.2808
      DO 20 J = 1,5
      GRIS = SQRT(31163189.8-(ALT-2011.7)**2)
      CALL SLAGRO(ISR,IGR,IELEV,INSRS,DELTA,
     1ALT,GRIS,SRIS,LIM)
      ALT = ALT+100.
   20 CONTINUE
      STOP
      END
C
C        Subroutine slagro, which converts slant
C           range data to ground range using
C           topographic data
C
      SUBROUTINE SLAGRO(ISR,IGR,IELEV,INSRS,
     1DELTA,ALT,GRIS,SRIS,LIM)
      DIMENSION IGR(1),ISR(1),INSRS(1),IELEV(1)
      DO 10 I1 = 1,LIM
      ARG1 = (GRIS+(I1-1)*DELTA)**2
      ARG2 = (ALT-IELEV(I1))**2
      SRDIST = SQRT(ARG1+ARG2)
      I2 = 1.5 + (SRDIST-SRIS)/DELTA
      IF(I2.GT.LIM.OR.I2.LT.1) GOTO 10
      IRDIST = SRDIST+1
      I2 = 1.5 + (IRDIST-SRIS)/DELTA
      DRDIST = SRDIST-IRDIST+1
      IGR(I1) = ISR(I2)+DRDIST*(ISR(I2+1)
     1-ISR(12))
C     IGR(I1) = ISR(I2)
C         INSRS is index number of slant range
C           sample, showing how it corresponds
C           to ground range.
```

```
C
      INSRS(I1) = I2
   10 CONTINUE
      RETURN
      END
```

APPENDIX D

FORTRAN PROGRAM
TO FIND RADAR BACKSCATTER
VS. ANGLE-OF-INCIDENCE

```
C         Program for backscatter curve
C         Ground range must be known to compute
C            gradient for each backscatter value
C         Finds backscatter of annulus
C
      SUBROUITINE BACSCA(IE,IR,ALPHA,RADAR)
      DIMENSION IE(100,100),IR(100,100),
     1ALPHA(10000),RADAR(10000)
C
C         IE  is  array with topographic data
C         IR  is  ground range image data
C         ALPHA  is  angle of incidence
C             (to be found)
C         RADAR  is  backscatter value
C             corresponding to angle
C
      DATA H,G,DEL,DEL2,OMEGA/6100.,3801.
     118,12.,24.,0./
      COSFLI = COS(OMEGA)
      SINFLI = SIN(OMEGA)
      ICOUNT = 0
      DO 30 J=1,93
      DO 30 I = 1,100
   30 IE(I,J) = IE(I,J)/3.2808
      DO 10 J = 1,93
      DO 10 I = 1,100
      RADI1=45-I
      RADI2 = 41-J
      TESDIS  = SQRT(RADI1*RADI1 +
     1RADI2*RADI2)
      IF(TESDIS.LT.21..OR.TESDIS.GT.35.) GOTO 10
      HE = H - IE(I,J)
      GX = G+ I*DEL
      PARZX = (IE(I+1,J)+IE(I+2,J) - IE(I-2,J) -
     1IE(I-1,J))/(2.*DEL2)
      PARZY = (IE(I,J+1)+IE(I,J+2) - IE(I,J-1)-
     1IE(I,J-2))/(2.*DEL2)
      A = SQRT(1. + PARZX*PARZX + PARZY*PARZY)
      B = SQRT(HE*HE + GX*GX)
      ICOUNT = ICOUNT + 1
      ALPHA(ICOUNT) = 57.295779*(ARCOS(ABS(-GX*
     1COSFLI*PARZX - GX*SINFLI*PARZY - HE)/(A*B)))
      RADAR(ICOUNT) = IR(I,J)
   10 CONTINUE
      END
```

APPENDIX E

FORTRAN PROGRAM
TO GENERATE PSEUDO-SAR IMAGES
IN GROUND RANGE AND SLANT RANGE
FROM TOPOGRAPHIC DATA

```
C          Program to generate ground range and
C             slant range pseudo-sar images from
C             topographic data
C          Uses approximated backscatter curve
C             found on SP mountain
C
      SUBROUTINE PSEUDO(ITOP,RADIM,SLARA,DIS)
      DIMENSION ITOP(100,100),RADIM(100,100),
     1SLARA(100,100),DIS(100,100),GRDIS(100,100)
C
C          ITOP is topographic data
C          RADIM  is  pseudo-image in ground range
C          SLARA  is  pseudo-image in slant range
C             (to be found)
C             (to be found)
C          DIS  is  slant range distance to
C             pseudo-vehicle
C          GRDIS  is  distance from groundtrack
C
      DELTA2 = 2.*DELTA
      COSFLI = COS(OMEGA)
      SINFLI = SIN(OMEGA)
      DO 10 J1 = 1,100
      DO 10 I1 = 1,100
      IF(ITOP(I1,J1).EQ.0)ITOP(I1,J1) = 6207
   10 ITOP(I1,J1) = ITOP(I1,J1)/3.2808
      DISTN = 10.E5
      DO 20 J = 2,99
      DO 20 I = 2,99
      AJ = J-1
      AI = I-1
      GAMMA = ATAN((AJ)/(AI))
      BI = I-1
      BJ = J-1
      D = SQRT(BI*BI+BJ*BJ)*DELTA
      ADGRIS = D*COS(OMEGA-GAMMA)
      GRDIS(I,J) = GRIS + ADGRIS
      H = ALT - ITOP(I,J)
      DIS(I,J) = SQRT(GRDIS(I,J)**2
     1+ H**2)
      IF(DIS(I,J).GT.DISTN) GOTO 70
      DISTN = DIS(I,J)
   70 CONTINUE
      PARZX = (ITOP(I+1,J) - ITOP(I-1,J))/DELTA2
      PARZY = (ITOP(I,J+1) - ITOP(I,J-1))/DELTA2
      A = SQRT(1. + PARZX*PARZX + PARZY*PARZY)
      B = DIS(I,J)
      ARG = ABS((GRDIS(I,J)*(PARZX*COSFLI +
     1PARZY*SINFLI)
     1+ H)/(A*B))
      ALPHA = 57.295779*ARCOS(ARG)
      IF(ALPHA.LT.17.) RADIM(I,J) = 99.
      IF(ALPHA.GE.80.) RADIM(I,J) = 22.
      IF(ALPHA.GE.17..AND.ALPHA.LT.32.) RADIM(I,J) =
```

```
     199.-2.467*(ALPHA - 17.)
      IF(ALPHA.GE.32..AND.ALPHA.LT.66.) RADIM(I,J) =
     162.-0.441*(ALPHA-32.)
      IF(ALPHA.GE.66..AND.ALPHA.LT.81.)RADIM(I,J) =
     147.-1.733*(ALPHA-66.)
 20   CONTINUE
      DO 80 J = 2,99
      DO 80 I = 2,99
      SLARA(I,J) = 20.
      I3 = ((DIS(I,J) - DISTN)*COSFLI/DELTA) + 2.5
      J3 = ((DIS(I,J) - DISTN)*SINFLI/DELTA) + 2.5
      IF(I3.LT.1.OR.I3.GT.100.OR.J3.LT.1.OR.J3.GT.100)
     1GO TO 80
      SLARA(I3,J3) = RADIM(I,J)
 80   CONTINUE
      RETURN
      END
```

APPENDIX F

FORTRAN PROGRAM
TO MEDIAN FILTER, APODIZE,
AND FIRST DIFFERENCE

```
C        Program for reading tape and median filtering
C
      LOGICAL*1 BYTE(2),BUF(512),TITLE(512)
      INTEGER*2 DATOUT(512,482),LEN,IBYTE
      EQUIVALENCE (BYTE,IBYTE)
      DIMENSION DATMED(128,128)
C        Zero out datmed:
      DO 60 J = 1,128
      DO 60 I = 1,128
   60 DATMED(I,J) = 0.
      LEN = 8
      CALL CNTRL('POSN=*4*',LEN,1)
      LEN = 512
      DO 10 J = 1,482
      CALL READ(BUF(1),LEN,0,LNUM,1)
      DO 20 I = 1,512
      IBYTE = 0
      BYTE(2) = BUF(I)
      DATOUT(I,J) = IBYTE
   20 CONTINUE
   10 CONTINUE
C        Do median filtering
C        Start counters for datmed array
      IJ = 0
      DO 40 J = 3,480,4
      IJ = IJ + 1
      II = 0
      DO 40 I = 3,500,4
      II = II + 1
      IMA = -300
      IMI = 300
      DO 50 L = 1,4
      DO 50 K = 1,4
      JL = J - 3 + L
      IK = I - 3 + K
      IF(DATOUT(IK,JL).GT.IMA) IMA = DATOUT(IK,JL)
      IF(DATOUT(IK,JL).LT.IMI) IMI = DATOUT(IK,JL)
   50 CONTINUE
      DATMED(II,IJ) = (IMA - IMI)/2.
   40 CONTINUE
C        Write out in packed form:
      LEN = 512
      DO 30 K = 1,128
   30 CALL WRITE(DATMED(1,K),LEN,0,0,2)
      STOP
      END
C     This program is in file REDAUTH
C     It includes a first difference filter and also
C          apodizes the data into a circle.
      DIMENSION DAT(128,128),DAT1(128,128)
      INTEGER*2 LEN/512/
      DO 10 I = 1,128
   10 CALL READ(DAT(1,I),LEN,0,LNUM,1)
C        Now do first difference filtering
```

```
C         Now do first difference filtering
      DO 20 J = 1,127
      DO 20 I = 1,127
   20 DAT1(I,J) = DAT(I,J+1) + DAT(I+1,J)-2.*DAT(I,J)
      DO 30 M = 1,128
   30 DAT1(128,M) = DAT1(127,M)
      DO 40 N = 1,128
   40 DAT1(N,128) = DAT1(N,127)
C         Now apodize to a circle around (64.,64.)
      DO 50 KK = 1,128
      AKK = KK
      DO 50 JJ = 1,128
      AJJ = JJ
   50 IF(SQRT((AKK-64.)**2 +
     1(AJJ-64.)**2).GT.63.) DAT1(JJ,KK) = 0.
C         Now write out the result
      DO 60 LL = 1,128
   60 CALL WRITE(DAT1(1,LL),LEN,0,0,2)
      STOP
      END
```

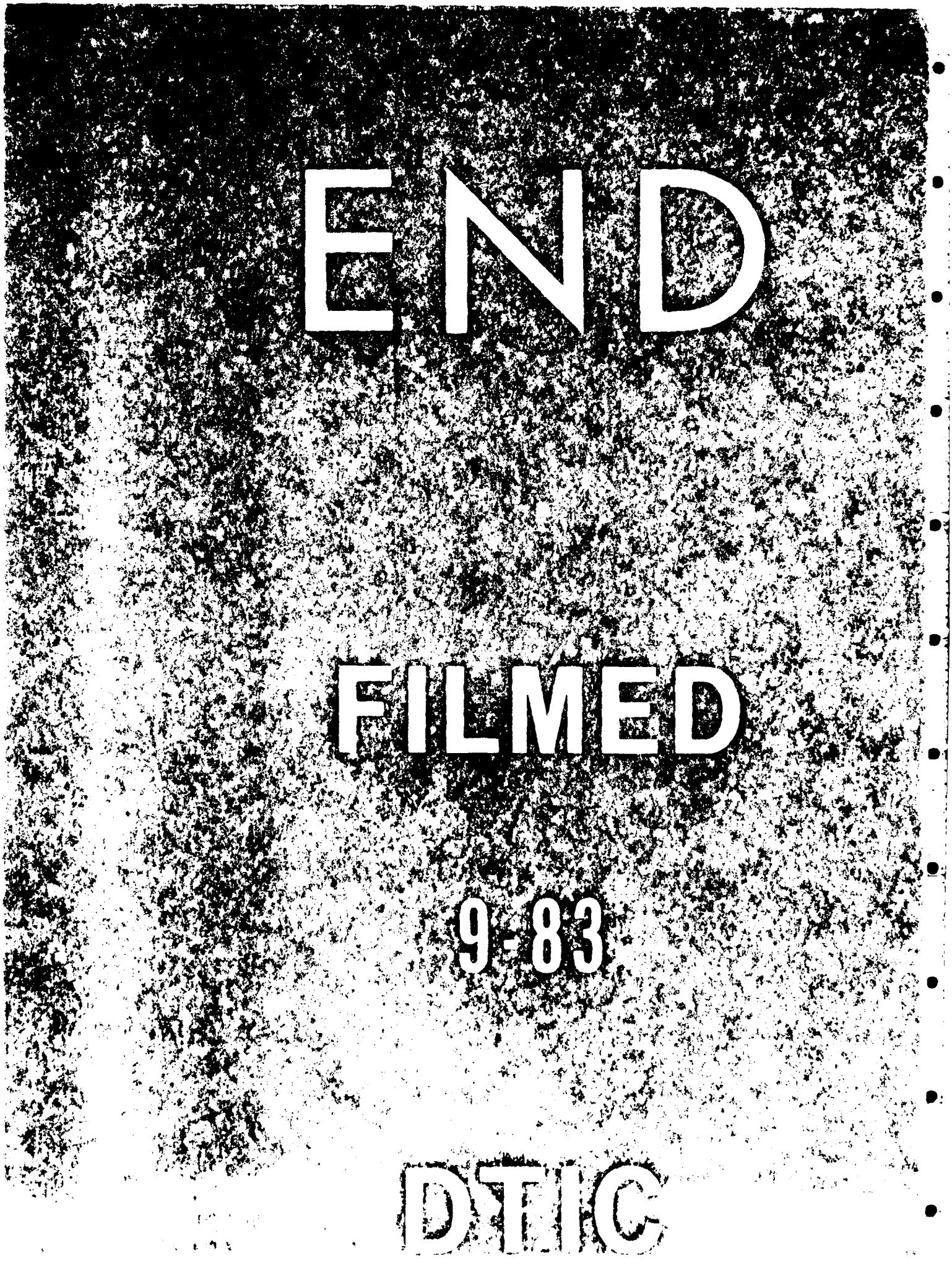
END
FILMED
9-83
DTIC